



ELSEVIER

Contents lists available at ScienceDirect

Developmental Biology

journal homepage: www.elsevier.com/locate/developmentalbiology

Compensatory embryonic response to allele-specific inactivation of the murine X-linked gene *Hcfc1*



Shilpi Minocha, Tzu-Ling Sung¹, Dominic Villeneuve, Fabienne Lammers, Winship Herr*

Center for Integrative Genomics, Génopode, University of Lausanne, 1015 Lausanne, Switzerland

ARTICLE INFO

Article history:

Received 27 November 2015

Received in revised form

22 February 2016

Accepted 22 February 2016

Available online 24 February 2016

Keywords:

Cell proliferation

HCF-1

Liver regeneration

Post-implantation development

X chromosome inactivation

ABSTRACT

Early in female mammalian embryonic development, cells randomly inactivate one of the two X chromosomes to achieve overall equal inactivation of parental X-linked alleles. *Hcfc1* is a highly conserved X-linked mouse gene that encodes HCF-1 – a transcriptional co-regulator implicated in cell proliferation in tissue culture cells. By generating a Cre-recombinase inducible *Hcfc1* knock-out (*Hcfc1*^{lox}) allele in mice, we have probed the role of HCF-1 in actively proliferating embryonic cells and in cell-cycle re-entry of resting differentiated adult cells using a liver regeneration model. HCF-1 function is required for both extraembryonic and embryonic development. In heterozygous *Hcfc1*^{lox/+} female embryos, however, embryonic epiblast-specific Cre-induced *Hcfc1* deletion (creating an *Hcfc1*^{epiKO} allele) around E5.5 is well tolerated; it leads to a mixture of HCF-1-positive and -negative epiblast cells owing to random X-chromosome inactivation of the wild-type or *Hcfc1*^{epiKO} mutant allele. At E6.5 and E7.5, both HCF-1-positive and -negative epiblast cells proliferate, but gradually by E8.5, HCF-1-negative cells disappear owing to cell-cycle exit and apoptosis. Although generating a temporary developmental retardation, the loss of HCF-1-negative cells is tolerated, leading to viable heterozygous offspring with 100% skewed inactivation of the X-linked *Hcfc1*^{epiKO} allele. In resting adult liver cells, the requirement for HCF-1 in cell proliferation was more evident as hepatocytes lacking HCF-1 fail to re-enter the cell cycle and thus to proliferate during liver regeneration. The survival of the heterozygous *Hcfc1*^{epiKO/+} female embryos, even with half the cells genetically compromised, illustrates the developmental plasticity of the post-implantation mouse embryo – in this instance, permitting survival of females heterozygous for an X-linked embryonic lethal allele.

© 2016 The Authors. Published by Elsevier Inc. This is an open access article under the CC BY-NC-ND license (<http://creativecommons.org/licenses/by-nc-nd/4.0/>).

1. Introduction

During animal development a totipotent zygote becomes a differentiated multicellular organism through regulated patterns of cell proliferation and differentiation, which themselves are controlled via programs of gene transcription. Chromatin is the structural basis by which the genome is packaged and genes are transcriptionally regulated. Transcriptional regulation involves physical association between sequence-specific DNA-binding proteins and chromatin-modifying enzymes, which in some cases is aided by protein adaptors that physically link these two classes of regulators. An example of the latter class is the human herpes simplex virus host-cell factor HCF-1 (for reviews see Kristie et al. (2010) and Zargar and Tyagi (2012)).

HCF-1 is a conserved metazoan protein. In mice and human, it

resides at the transcriptional start sites of many genes (e.g., 743 in embryonal stem cells and over 5000 in HeLa cells; (Dejosez et al., 2010; Michaud et al., 2013)) and associates with both sequence-specific DNA-binding proteins (e.g., E2F1 and E2F4, Thap11/Ronin, ZNF143) and chromatin-modifying enzymes (e.g., MLL and Set1 histone H3 Lysine 4 methyltransferases and Sin3 histone deacetylase) (for review see Zargar and Tyagi (2012)). Genetic studies in mammalian cell culture have shown that HCF-1 is important for multiple aspects of cell proliferation (Goto et al., 1997; Julien and Herr, 2003; Reilly and Herr, 2002). For example, temperature-sensitive tsBN67 cells, which carry a point mutation in the hamster gene encoding HCF-1, exit from the cell-division cycle in the G1 phase when transferred from 33.5 °C to 40 °C – but not immediately, rather after about two rounds of cell division (Goto et al., 1997).

Here, we study the cell proliferation and developmental roles of HCF-1 in mice. The mouse gene encoding HCF-1 is called *Hcfc1* and resides on the X chromosome (Frattini et al., 1996; Kristie, 1997), and as such is subject to transcriptional silencing via

* Corresponding author.

E-mail address: winship.herr@unil.ch (W. Herr).

¹ Present address: Academia Sinica, 128 Academia Road, Taipei, Taiwan.

X-chromosome inactivation. X-chromosome inactivation in female mammals occurs in two waves – imprinted followed by random inactivation: (i) in the imprinted form, soon after fertilization, there is exclusive inactivation of the paternally inherited X (Xp) chromosome such that only the maternally inherited X (Xm) chromosome is active in both embryonic and extraembryonic tissues; (ii) in the random form, the Xp chromosome is reactivated around the time of implantation in the embryonic tissue exclusively and either X chromosome is subsequently randomly inactivated (for reviews, see Augui et al. (2011) and Heard and Disteché (2006)).

In heterozygous cells, random X-chromosome inactivation can be used to study the activity of wild-type and mutant alleles separately but in side-by-side cells. Here, we used this property, combined with the generation of a conditional mouse *Hcfc1* knock-out allele (*Hcfc1*^{CKO}), to study the role of HCF-1 in embryonic and extraembryonic as well as adult tissues. The results reveal essential but differing embryonic and adult roles of HCF-1 in cell proliferation. They illustrate as well high plasticity in post-implantation development as wild-type embryonic cells can fully compensate for the loss of proliferative potential in their HCF-1-negative cohorts.

2. Materials and methods

2.1. Mice

All experimental studies have been performed in compliance with the EU and national legislation rules, as advised by the Le-manique Animal Facility Network (Resal), concerning ethical considerations of transportation, housing, strain maintenance, breeding and experimental use of animals.

Mice bearing the *Hcfc1* conditional (lox) allele were generated by Ozgene Pty Ltd. The targeting vector contained a 10 kb genomic sequence of part of the *Hcfc1* gene and its upstream sequence. Briefly, an 870 bp PCR product containing *Hcfc1* exons 2 and 3 and their flanking intron sequences was amplified from C57BL/6 genomic DNA and cloned into pPCR. The forward primer was designed to include a loxP site (5' loxP) for Cre-induced recombination and the reverse primer a *PacI* site for subsequent cloning. A PGK-Neo-SD-IS cassette flanked by FRT sites containing a second loxP site (3' loxP) at the 3' end was inserted into the *PacI* site. For homologous recombination, a 5.2 kb fragment upstream of exon 2 was inserted before the 5' loxP site and a 3.9 kb fragment downstream of exon 3 was inserted after the 3' loxP site. With this construct a homologously recombined male C57BL/6 embryonic-stem cell line was isolated and successfully used to create a mosaic mouse for successful germ-line transmission. The official name for the resulting mouse allele is *B6-Hcfc1tm1^{Lwh}* according to the guidelines by Mouse Genome Informatics (MGI, The Jackson Laboratory) but it is referred to here as *Hcfc1*^{lox}. The *Hcfc1*^{lox} allele contains two loxP sites, one in intron 1 and another in intron 3, and can undergo recombination in the presence of Cre recombinase. Cre-recombinase-induced deletion of exons 2 and 3 resulted in splicing of exons 1 and 4 as determined by RNA-sequence analysis (see tamoxifen induction below).

Other strains used in this study include wild-type C57BL/6 mice and C57BL/6 mice carrying the *Sox2Cre*^{tg} (Hayashi et al., 2002), *CAG-EGFP*^{tg} (Hadjantonakis et al., 1998), and *Alb-Cre-ERT2*^{tg} ((Schuler et al., 2004); a gift from Dr. Daniel Metzger, IGBMC Strasbourg) transgenes.

Females and littermate males were housed four to five per cage at 23 °C, with a 12:12 h light–dark cycle and *ad libitum* access to water and food.

2.2. DNA isolation and genotyping

For genotyping, genomic DNA was isolated from mouse ear tags for postnatal mice or entire conceptus for whole embryos as previously described (Truett et al., 2000). For paraffin-embedded embryo sections, DNA for genotyping was extracted by (i) preferential scraping of the epiblast region of 3–4 sections with a surgical blade, (ii) transferring the scraped sections into an eppendorf tube, and (iii) deparaffinizing and xylene removal as described (Gohar and Mohammadi, 2009). Subsequent DNA extraction was done as described (Truett et al., 2000). Samples were used for PCR amplification with specific primer sets using the KAPA2G Fast HotStart Genotyping PCR Mix (cat no. KK5621). The annealing was done at 62 °C for 15 s with an extension at 72 °C for 10 s.

Primers for genotyping are listed below.

For HCF-1: p1 (5'-GGAGGAACATGAGCTTTAGG-3'), p2 (5'-CAATAGGCCGAGTACCATCACAC-3'), and p3 (5'-GGGAAAGTAGCCACTCTG-3').

For Cre: Sense (5'-AGGTGTAGAGAAGGCACTTAGC-3') and Anti-sense (5'-CTAATCGCCATCTTCCAGCAGG-3') (Le and Sauer, 2000).

For Y chromosome: Sry-1 (5'-AACAACTGGGCTTGCACATTG-3') and Sry-2 (5'-GTTTATCAGGGTTTCTCTAGC-3') (Steele-Perkins et al., 2005).

For GFP: oIMR0872 (5'-AAGTTCATCTGCACCACCG-3') and oIMR1416 (5'-TCCTTGAAGAAGATGGTGCG-3').

2.3. Tamoxifen induction

Control *Hcfc1*^{lox/+} and test *Alb-Cre-ERT2*^{tg}; *Hcfc1*^{lox/+} adult mice (10–14 weeks old) were administered intraperitoneal injections of 1 mg/mouse tamoxifen [100 µl of 10 mg/ml (1:10 ethanol: corn oil); Sigma-Aldrich CAS#10540-29-1] four times every 24 h starting on Day 0. High-throughput RNA-sequence analysis showed that the tamoxifen-induced hepatic *Hcfc1*^{hepKO} deletion in *Alb-Cre-ERT2*^{tg}; *Hcfc1*^{hepKO/+} mice led to splicing of *Hcfc1* exon 1 to exon 4.

2.4. BrdU incorporation

To label embryonic cells in S phase, pregnant mice were injected intraperitoneally with the cell-proliferation marker, 5-bromo-2'-deoxyuridine (BrdU; BD Biosciences, cat. # 550891) to a final concentration of 50 mg/kg body weight, sacrificed 6 h post-injection, and BrdU incorporation revealed by immunofluorescence staining (see below).

2.5. Tissue histology and immunohistochemistry

Intact embryonic day (E) 6.5 to E8.5 embryos were paraffin-embedded and sectioned within their decidua along a sagittal axis to generate 4 µm thick sections using a microtome (MICROM HM325). Similarly, paraffin-embedded E12.5 embryos, and post-natal (P) 0 and P5 brain and liver tissue samples were also sliced at 4 µm thickness. Early postnatal and adult brain and liver samples were cut with the help of a cryostat microtome (MICROM HM550) to generate 20 µm thick cryo-sections.

Paraffin-embedded sections were (i) deparaffinized in xylene, (ii) rehydrated through graded alcohol washes, (iii) rinsed twice with PBS, (iv) antigen revealed by heating in a 750 W microwave oven until boiling (approximately 10 min) in citrate buffer (10 mM, pH 6.0), (v) allowed to slowly cool down at 4 °C, (vi) washed twice with PBS, and (vii) blocked for 30 min with 2% normal goat serum (NGS) (Sigma-Aldrich, cat. #G9023) in PBS at room temperature (RT).

Cryo-sections were (i) dried for 10 min, (ii) fixed for 10 min

with 4% paraformaldehyde (Electron Microscopy Sciences, CAS #30525-89-4) at 4 °C, (iii) washed thrice with PBS, (iv) permeabilized for 10 min with 0.3% Triton X-100 in PBS, (v) washed thrice with PBS, and (vi) blocked for 1 h with 2% NGS in PBS at RT.

After blocking, immunohistochemistry of both paraffin- and cryo-sections was performed similarly by (i) incubation of the slices with specific primary antibody diluted in 2% NGS overnight at 4 °C, (ii) three washes with PBS, (iii) incubation with secondary antibody for 30 min in the dark at RT, (iv) three washes with PBS, (v) counterstaining with 4',6-diamidino-2-phenylindole (DAPI) (Sigma-Aldrich, CAS # 28718-90-3), (vi) two washes with PBS, (vii) embedding with Mowiol mounting medium (Sigma-Aldrich, CAS # 9002-89-5), and (viii) analyzed using an AxioImager M1 microscope with AxioCam MRm monochrome and AxioCam MRc color cameras (Carl Zeiss AG, Oberkochen, Germany) and a Zeiss CLSM 710 spectral confocal laser scanning microscope. Images were processed using AxioVision 4.8.2 (Carl Zeiss AG, Oberkochen, Germany) and Imaris 8.2 (Bitplane Inc.) software. Immunohistochemistry of whole mount embryos was done as described previously (Joyner and Wall, 2008).

Primary antibodies used were: rabbit anti-HCF-1 (1:1000, H12, (Wilson et al., 1993)), rat anti-Ki67 (1:60, eBioscience cat. # 41-5698), anti-HNF4 α (1:100, R&D Systems cat. # PP-H1415-00) and anti-PCNA (1:50, BD Transduction Laboratories cat. # 610665) mouse monoclonal antibodies, rabbit anti-Histone H3 phospho Ser10 (1:100, Abcam cat. # ab5176), rabbit anti-Oct4 (1:250, Abcam cat. # ab19857), and chicken anti-GFP (1:500, Aves Labs, Inc. cat. # GFP-1020).

Secondary antibodies used were: goat anti-rabbit Alexa 488 (1:400, Molecular Probes cat. # A11034), goat anti-mouse Alexa 568 (1:500, Molecular Probes cat. # A11019), goat anti-rabbit Alexa 568 (1:1000, Molecular Probes cat. # A21069), goat anti-mouse Alexa 488 (1:400, Molecular Probes cat. # A11029), donkey anti-mouse Alexa 594 (1:500, Molecular Probes cat. # A11005), and goat anti-mouse Alexa 635 (1:300, Molecular Probes cat. # A31575).

2.6. TUNEL assay

Terminal deoxynucleotidyltransferase-mediated dUTP-biotin nick end labeling (TUNEL) was performed on paraffin-embedded embryo sections with the *in situ* cell death detection kit (Roche Applied Science, product # 11684795910), according to the manufacturer directions.

2.7. Partial hepatectomy

2/3 or 70% partial hepatectomy (PH) was performed as described (Mitchell and Willenbring, 2008).

2.8. Measurement of body composition by EchoMRI

Total body fat, lean mass, free liquids, and total body water of live mice were measured with EchoMRI™-100H body composition analyzer under isoflurane anesthesia.

2.9. Quantitation and statistical analyses

For Supplemental Tables 1 and 3, cells in the entire embryonic region of single 4 μ m-thick paraffin sections were counted. For Supplemental Table 4, for each liver studied, all cells in a representative field of a 4 μ m-thick paraffin section were counted. Both χ^2 tests and Student's *t*-tests were performed by using the R package (www.r-project.org).

3. Results

3.1. Generation of the *Hcfc1*^{ckO} allele

Fig. 1A shows a schematic of the wild-type mouse HCF-1 protein (a), and a description of the genesis of the ckO *Hcfc1*^{ckO} allele (b–d) along with its hypothetical truncated HCF-1 product (e). The mouse *Hcfc1* gene consists of 26 exons spread over 25 kb (Fig. 1Ab; Kristie, 1997). We designed and obtained (see Section 2) a C57BL/6 *Hcfc1* allele, called *Hcfc1*^{lox}, with individual loxP sites flanking exons 2 and 3 (Fig. 1Ac) for Cre recombinase-mediated exon2/3 deletion generating the *Hcfc1*^{ckO} allele (Fig. 1Ad). Pre-mRNA splicing of the remaining *Hcfc1*^{ckO} exons 1 and 4 (see Section 2) generates an mRNA in which the reading frame goes out of frame for 2 codons (encoding Gly-Thr) before encountering a termination codon (Fig. 1Ae). The predicted truncated protein is 66 amino acids long and unable to make even a single β -stranded blade of the predicted HCF-1_{KEL} Kelch-domain β -propeller structure (Wilson et al., 1997) – it is unlikely to possess any wild-type HCF-1 functions.

Fig. 1B shows how we differentiated between the three *Hcfc1*⁺, *Hcfc1*^{lox} and *Hcfc1*^{ckO} alleles by PCR amplification with a mix of the three oligonucleotide primers p1, p2, and p3 generating three different amplification products: 476, 551 and 347 bp, respectively. Note that, for the *Hcfc1*⁺ and *Hcfc1*^{lox} alleles, larger p1/p3 amplification products of 1053 or 1272 bp, respectively, spanning exons 2 and 3 were not observed under our PCR conditions.

To genotype individuals, as shown in Fig. 1C, we analyzed the *Hcfc1*-allele status (top), and the presence or absence of the Cre transgene (middle) and Y chromosome (bottom). In the absence (lanes 1 and 2) or presence (lanes 5 and 6) of an active Cre transgene (here *Sox2Cre*^{tg}; see below), DNA isolated from wild-type *Hcfc1*⁺ male (lanes 1 and 5) or female (lanes 2 and 6) offspring resulted in the generation of the wild-type 476 bp (+) fragment. In the absence of a Cre transgene, a hemizygous *Hcfc1*^{lox/Y} male (lane 3) and heterozygous *Hcfc1*^{lox/+} female (lane 4) generated the expected 551 bp loxP-specific (lox) fragment in the absence (hemizygous male) or presence (heterozygous female) of the wild-type 476 bp fragment. The presence of a Cre transgene, however, resulted in a heterozygous *Hcfc1*^{lox/+} female being converted to a heterozygous *Hcfc1*^{ckO/+} female that generated the *Hcfc1*^{ckO} allele-specific product of 347 bp (ckO; lane 7). (Note that there were no *Hcfc1*^{ckO/Y} male offspring – see below.) The accuracy of the Cre recombinase-induced loxP recombination deleting *Hcfc1* exons 2 and 3 was verified by DNA-sequence analysis (data not shown).

The availability of mice carrying the *Hcfc1*^{lox} allele permitted us to study *Hcfc1* function under a number of diverse conditions. Table 1 describes the terminology for the different *Hcfc1* alleles generated for this study: by using different sources of Cre recombinase, we generated the *Hcfc1*^{ckO} allele under three different conditions: (i) in the embryonic epiblast in combination with an autosomal *Sox2Cre*^{tg} transgene (Hayashi et al., 2002, 2003) – we refer to this allele as *Hcfc1*^{epiKO}, (ii) in adult liver hepatocytes in combination with a tamoxifen-inducible *Alb-Cre-ERT2*^{tg} transgene (Schuler et al., 2004) – we refer to this allele as *Hcfc1*^{hepKO}, and (iii) specifically on the paternally inherited Xp chromosome (see below) – we refer to this allele as *Hcfc1*^{XpKO}. A fourth allele, representing a maternally inherited X-linked *Hcfc1*^{epiKO} allele, is referred to as *Hcfc1*^{XmKO}.

3.2. Broad *Hcfc1* expression in mouse tissues

Before analyzing the effects of *Hcfc1* inactivation, we assayed *Hcfc1* expression in the mouse. The human *HCFC1* gene is highly expressed in actively dividing cells in culture and in fetal and

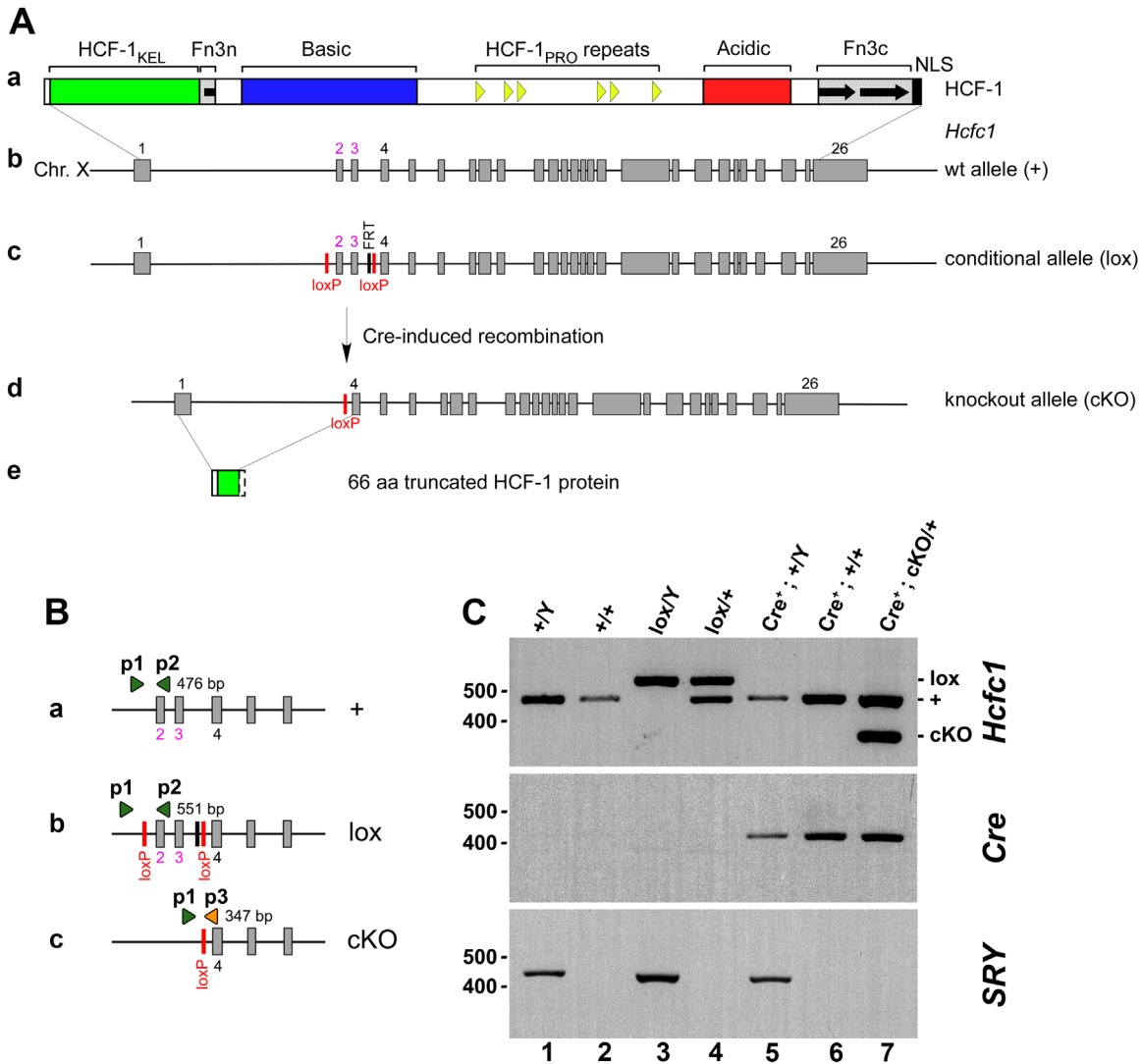


Fig. 1. Generation of an *Hcfc1* conditional knockout allele in mice. (A) Schematic representation of the mouse HCF-1 protein and *Hcfc1*^{CKO} allele generation. (a) HCF-1 elements represent a Kelch domain (HCF-1_{KEL}); basic and acidic regions enriched in basic and acidic residues, respectively; six proteolytic processing repeats (HCF-1_{PRO}); two fibronectin type 3 repeats (HCF-1_{Fn3}) formed from N- (Fn3n) and C- (Fn3c) terminal segments (Park et al., 2012); and a C-terminal nuclear localization signal (NLS). (b) The wild-type (wt) murine *Hcfc1* allele (+) consists of 26 exons spanning 25 kb on the X chromosome. (c) The *Hcfc1* conditional allele (lox) contains loxP sites before exon 2 and after exon 3. (d) The presence of Cre protein results in the generation of the conditional knockout (cKO) allele. (e) The cKO allele results in exon 1 to exon 4 splicing, which predicts the synthesis of a 66 amino acid truncated HCF-1 protein. FRT: residual sequence remaining from removal of the selection marker in embryonic stem cells before generation of the mice. (B) (a) Wild-type (+), (b) lox, and (c) cKO *Hcfc1* alleles can be distinguished by PCR using the primer pairs (p1, p2, and p3) indicated. Predicted fragment sizes are indicated. (C) Electrophoretic separation of PCR products of wt *Hcfc1*^{+/Y} male (lane 1), wt *Hcfc1*^{+/+} female (lane 2), *Hcfc1*^{lox/Y} male (lane 3), *Hcfc1*^{lox/+} female (lane 4), *Sox2Cre*^{tg}; *Hcfc1*^{+/Y} male (lane 5); *Sox2Cre*^{tg}; *Hcfc1*^{+/+} female (lane 6); and *Sox2Cre*^{tg}; *Hcfc1*^{CKO/+} heterozygous female (lane 7) to analyze the *Hcfc1*-allele status (top), and the presence or absence of the Cre transgene (middle) or Y chromosome (bottom).

Table 1
Description of *Hcfc1* alleles used in this study.

Alleles	Description
<i>Hcfc1</i> ⁺	Wild-type
<i>Hcfc1</i> ^{lox}	<i>Hcfc1</i> gene containing loxP sites flanking exons 2 and 3 for induced knockout by Cre recombinase
<i>Hcfc1</i> ^{CKO}	Conditional knock-out of the <i>Hcfc1</i> ^{lox} allele by Cre recombinase
<i>Hcfc1</i> ^{epiKO}	Epiblast-specific <i>Hcfc1</i> knockout induced by paternal Ap <i>Sox2Cre</i> ^{tg} and maternal Xm <i>Hcfc1</i> ^{lox} inheritance
<i>Hcfc1</i> ^{hepKO}	Liver hepatocyte-specific <i>Hcfc1</i> knockout by tamoxifen-induced <i>Alb-Cre-ERT2</i> ^{tg} and <i>Hcfc1</i> ^{lox} inheritance
<i>Hcfc1</i> ^{XpKO}	Xp-specific <i>Hcfc1</i> knockout induced by maternally inherited Cre recombinase resulting from a female <i>Sox2Cre</i> ^{tg} ; <i>Hcfc1</i> ^{epiKO/+} and male <i>Hcfc1</i> ^{lox/Y} cross
<i>Hcfc1</i> ^{XmKO}	Maternally inherited (Xm) <i>Hcfc1</i> ^{epiKO} allele

placental tissues (Wilson et al., 1995); it continues to be expressed in adult tissues, comprising mostly quiescent cells, though the levels are comparatively reduced (Huang et al., 2012; Wilson et al., 1995). Here, we investigated the levels and subcellular localization of mouse HCF-1 by immunostaining wt and *Hcfc1*^{lox/Y} male

embryos and postnatal tissues. HCF-1 was ubiquitous and predominantly nuclear in (i) *Hcfc1*^{lox/Y} embryonic day (E) 2.5 and 3.0 blastomeres (Supplemental Fig. 1A and B), (ii) wt and *Hcfc1*^{lox/Y} E6.5–E8.5 embryos (Supplemental Figs. 1 and 2C–E), (iii) *Hcfc1*^{lox/Y} E9.5 and E12.5 embryos (Supplemental Fig. 3A and B), and (iv)

brain and liver tissue at postnatal day 0 (P0) and from 10-week old young adults (Supplemental Fig. 3C–F). Consistent with our inability to observe any abnormal phenotype in *Hcfc1*^{lox/Y} mice (see below), the staining and localization of HCF-1 were identical in wt and *Hcfc1*^{lox/Y} mice (compare Supplemental Figs. 1 and 2). The broad pattern of *Hcfc1* expression suggests that HCF-1 plays roles in both proliferating and non-proliferating cells.

3.3. Complete embryonic loss of HCF-1 is lethal

Initial crosses between *Hcfc1*^{lox} mice and the OzCre mouse strain homozygous for a Cre transgene driven by the PGK promoter (Ozgene, Perth, Australia) failed to generate progeny carrying the *Hcfc1*^{ckO} allele. Given the very early onset of PGK expression during embryonic development (McBurney et al., 1994), we asked whether later epiblast-specific *Hcfc1* deletion might lead to viable offspring, by crossing heterozygous *Sox2Cre*^{tg} males (tg for transgene) and homozygous *Hcfc1*^{lox/lox} females. *Sox2Cre*^{tg} mice carry an autosomal Cre transgene that, when paternally inherited, directs an onset of Cre recombinase synthesis around E4.5 exclusively in the post-implantation epiblast (Hayashi et al., 2002, 2003).

A cross between *Hcfc1*^{lox/lox} females and heterozygous *Sox2Cre*^{tg} males will result in both *Hcfc1*^{lox/Y} male and *Hcfc1*^{lox/+} female zygotes, either with or without the *Sox2Cre* transgene. Only *Hcfc1*^{lox/Y} male zygotes with the *Sox2Cre*^{tg} allele can generate a complete epiblast-specific *Hcfc1*^{epiKO} deletion during embryonic development; heterozygous *Hcfc1*^{lox/+} female zygotes with the *Sox2Cre*^{tg} allele are instead expected to generate a heterozygotic epiblast-specific *Hcfc1*^{epiKO} deletion.

To test the efficacy and timing of *Sox2Cre*^{tg}-induced *Hcfc1*^{lox} to *Hcfc1*^{epiKO} conversion, we probed, as shown in Fig. 2, E5.5 littermate *Hcfc1*^{lox/Y} embryos carrying or not the *Sox2Cre*^{tg} transgene for the presence of the *Hcfc1*^{epiKO} allele by PCR (Fig. 2B) and HCF-1 protein by immunostaining (Fig. 2A). Already at E5.5, in the presence of the *Sox2Cre*^{tg} transgene (lane 2, Fig. 2B, middle), the *Hcfc1*^{epiKO} allele is evident (lane 2, Fig. 2B, top; red arrowhead); immunostaining showed that, in contrast to the *Hcfc1*^{lox/Y} embryo lacking the *Sox2Cre*^{tg} transgene where all cells are HCF-1 positive, in the presence of the *Sox2Cre*^{tg} transgene two-thirds of epiblast cells are already depleted for HCF-1 (Fig. 2C and Supplemental Table 1). These results are consistent with initiation of the *Sox2Cre*^{tg}-transgene mediated *Hcfc1*^{epiKO} allele generation before

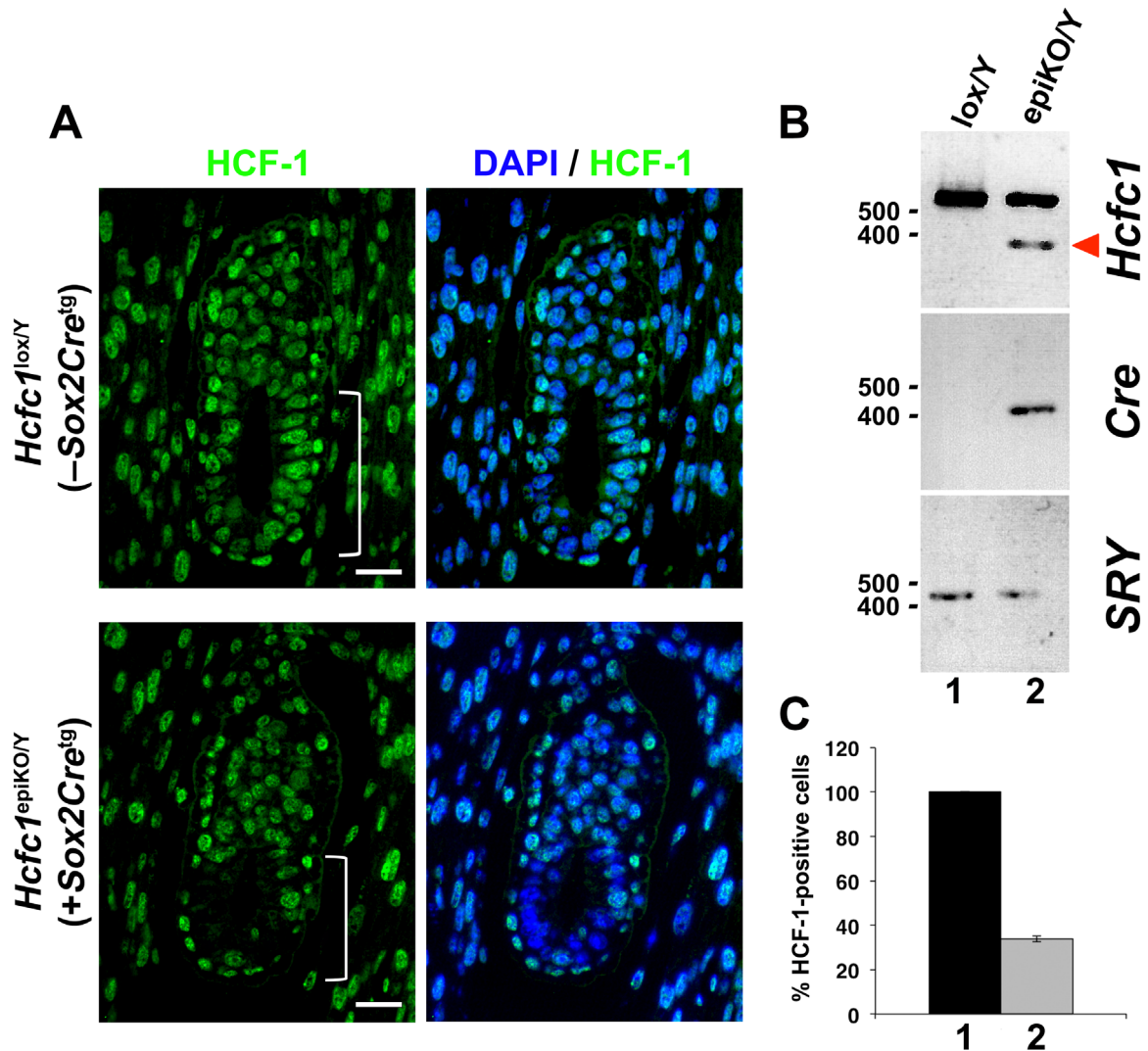


Fig. 2. Epiblast-specific depletion of HCF-1 is evident at E5.5. (A) Immunofluorescence analysis of paraffin-embedded sections of control *Hcfc1*^{lox/Y} and *Sox2Cre*^{tg}; *Hcfc1*^{epiKO/Y} male embryos at E5.5. Immunostaining was performed with anti-HCF-1 antibody (green) and DAPI (blue). The square brackets mark the epiblast region. Scale bar: 25 μm for all panels. (B) Electrophoretic separation of PCR products of control *Hcfc1*^{lox/Y} (lane 1) and *Sox2Cre*^{tg}; *Hcfc1*^{epiKO/Y} (lane 2) male embryos to analyze the *Hcfc1*-allele status (top), and the presence or absence of the *Cre* transgene (middle) and Y chromosome (bottom). The arrowhead indicates the epiKO allele-specific cKO PCR product of 347 bp. (C) Graph showing the percentage of HCF-1-positive cells in control *Hcfc1*^{lox/Y} ($n=6$; bar 1) and *Sox2Cre*^{tg}; *Hcfc1*^{epiKO/Y} ($n=3$; bar 2) male embryos at E5.5.

Table 2
Progeny of *Hcfc1*^{lox/lox} females crossed with heterozygous *Sox2Cre*^{tg} males.

F1 Progeny			Number of progeny obtained at	
Original <i>Hcfc1</i> genotype	<i>Sox2Cre</i> transgene	Epiblast Cre-mediated <i>Hcfc1</i> genotype	Birth	E12.5
<i>Hcfc1</i> ^{lox/+}	–	<i>Hcfc1</i> ^{lox/+}	49	11
<i>Hcfc1</i> ^{lox/+}	+	<i>Hcfc1</i> ^{epiKO/+}	43	10
<i>Hcfc1</i> ^{lox/Y}	–	<i>Hcfc1</i> ^{lox/Y}	51	9
<i>Hcfc1</i> ^{lox/Y}	+	<i>Hcfc1</i> ^{epiKO/Y}	0	10 ^a
Total embryos analyzed			143	40

^a Sites of resorption.

E5.5, giving time for depletion of HCF-1 in the majority of epiblast cells by E5.5.

As shown in Table 2, we analyzed the *Hcfc1*⁺ status of 143 newborn mice of the *Hcfc1*^{lox/lox} female crossed with heterozygous *Sox2Cre*^{tg}; *Hcfc1*^{+^Y} males by PCR. *Hcfc1*^{lox/+} females and *Hcfc1*^{lox/Y} males lacking the *Sox2Cre*^{tg} allele were equally well represented (49 and 51, respectively; *p*-value 0.8) among the offspring. Among the offspring carrying the *Sox2Cre*^{tg} allele, however, there were no *Hcfc1*^{lox/Y} or *Hcfc1*^{epiKO/Y} male offspring (*p*-value 1.6×10^{-10}). This result could be explained if the *Sox2Cre*^{tg} transgene is 100% efficient at inducing *Hcfc1*^{lox} to *Hcfc1*^{epiKO} allele conversion and the *Hcfc1*^{epiKO} allele is subsequently lethal in male embryos. To investigate this possibility, we analyzed embryos from the *Hcfc1*^{lox/lox} and heterozygous *Sox2Cre*^{tg/+}; *Hcfc1*^{+^Y} male crosses at E12.5 *in utero*. Indeed, *Hcfc1*^{epiKO/Y} male embryos were found at resorption sites (Table 2; Supplemental Fig. 4A), indicating embryonic lethality. Isolation of E9.5 embryos by dissection identified *Hcfc1*^{epiKO/Y} embryos that were exceptionally smaller in size and morphologically abnormal compared to control *Hcfc1*^{lox/Y} and *Hcfc1*^{lox/+} – and heterozygous *Hcfc1*^{epiKO/+} (see below) – littermate embryos (Supplemental Fig. 4B). Thus, epiblast-specific loss of *Hcfc1* function in males results in an embryonic lethality between E5.5 (see Fig. 2A) and E9.5 – this lethality is not explored further here.

In contrast to the male offspring, female offspring listed in Table 2 carrying the *Sox2Cre*^{tg} allele were obtained in numbers similar to *Sox2Cre*^{tg}-negative males and females (43 vs 51 and 49;

p-value 0.4 and 0.5, respectively). All of these *Sox2Cre*^{tg}-positive female offspring were *Hcfc1*^{epiKO/+} heterozygotes (compare lanes 6 and 7, Fig. 1C) lacking the *Hcfc1*^{lox} allele, indicating that here the Cre recombinase-induced epiblast-specific deletion of the X-linked *Hcfc1*^{lox} allele was completely penetrant. Together these results indicate that epiblast-specific *Hcfc1*^{epiKO/+} deletion on the maternal Xm chromosome can be both efficient and non-deleterious for long-term viability. Indeed the *Sox2Cre*^{tg}; *Hcfc1*^{epiKO/+} female offspring, although exhibiting marginal (albeit significant, *p*-value < 0.05) differences in body length and lean mass (Supplemental Fig. 5), remained healthy beyond 1 year and were fertile.

3.4. A maternally inherited *Hcfc1*^{XmKO} allele is lethal

We used the fertile *Sox2Cre*^{tg}; *Hcfc1*^{epiKO/+} females to study the requirements for HCF-1 function early in development, taking advantage of the differential activation/inactivation of the maternal Xm and paternal Xp inherited X-chromosomes post fertilization (see Section 1). Table 3 summarizes the results of these experiments. We performed four different crosses with all possible combinations of *Hcfc1*^{lox/+} and *Sox2Cre*^{tg}; *Hcfc1*^{epiKO/+} females, and *Hcfc1*^{+^Y} and *Hcfc1*^{lox/Y} males. To ensure that embryos defective in early development would be identified in the analysis, we examined and genotyped, in addition to perinatal mice, embryos at E7.5. As expected, *Hcfc1*^{lox/+} females crossed with either *Hcfc1*^{+^Y} or *Hcfc1*^{lox/Y} males produced an approximate Mendelian 1:1:1:1 ratio of the four possible sex-linked genotypes (data not shown). In contrast, as shown in Table 3, *Sox2Cre*^{tg}; *Hcfc1*^{epiKO/+} females crossed with either *Hcfc1*^{+^Y} (Cross 1) or *Hcfc1*^{lox/Y} (Cross 2) males gave more complex viability outcomes.

Cross 1 (*Sox2Cre*^{tg}; *Hcfc1*^{epiKO/+} × *Hcfc1*^{+^Y}) tests whether an *Hcfc1*^{KO} allele inherited on the Xm chromosome (*Hcfc1*^{XmKO}; see Table 1) can give rise to progeny (see Supplemental Table 2 for a description of the *Hcfc1* allele outcomes of Crosses 1 and 2). Indeed, it cannot as the only normal embryos or pups obtained in this cross were either *Hcfc1*^{+^Y} males or *Hcfc1*^{+^Y} females (Table 3, columns 1 and 3; *p*-value 6.7×10^{-8}). Given the *Hcfc1*^{epiKO/Y} lethality described in Table 2, the absence of *Hcfc1*^{XmKO/Y} male embryos or pups lacking a wild-type *Hcfc1*⁺ allele was to be expected (column 2). Here, however, whereas heterozygous *Hcfc1*^{epiKO/+} embryos and pups were viable in Table 2,

Table 3
The *Hcfc1*^{KO} allele is lethal when transmitted through the maternally inherited X^M chromosome but not when generated de novo on the paternally inherited X^P chromosome upon fertilization.

No.	Cross ^a	Age	1	2	3	4	5	6	Total
			<i>Hcfc1</i> ^{+^Y}	<i>Hcfc1</i> ^{XmKO/Y}	<i>Hcfc1</i> ^{+^Y}	<i>Hcfc1</i> ^{XmKO/+}	<i>Hcfc1</i> ^{+^Y} /XpKO	<i>Hcfc1</i> ^{XmKO/XpKO}	
1	♀ <i>Sox2Cre</i> ^{tg} ; <i>Hcfc1</i> ^{epiKO/+} X ♂ <i>Hcfc1</i> ^{+^Y}	E7.5	8	0	8	10 ^b	N/A	N/A	26
		P0	11	0	9	0			20
2	♀ <i>Sox2Cre</i> ^{tg} ; <i>Hcfc1</i> ^{epiKO/+} X ♂ <i>Hcfc1</i> ^{lox/Y}	E7.5	14	0	N/A	N/A	9 ^c	0	23
		P0	10	0			6	0	16

^aMaternal and paternal parent of origin of X chromosome-linked alleles are indicated in red and blue, respectively.

^bAbnormal embryos shown in Fig. 3.

^cNormal embryos shown in Fig. 4.

N/A not applicable, genotypes not possible from the listed cross.

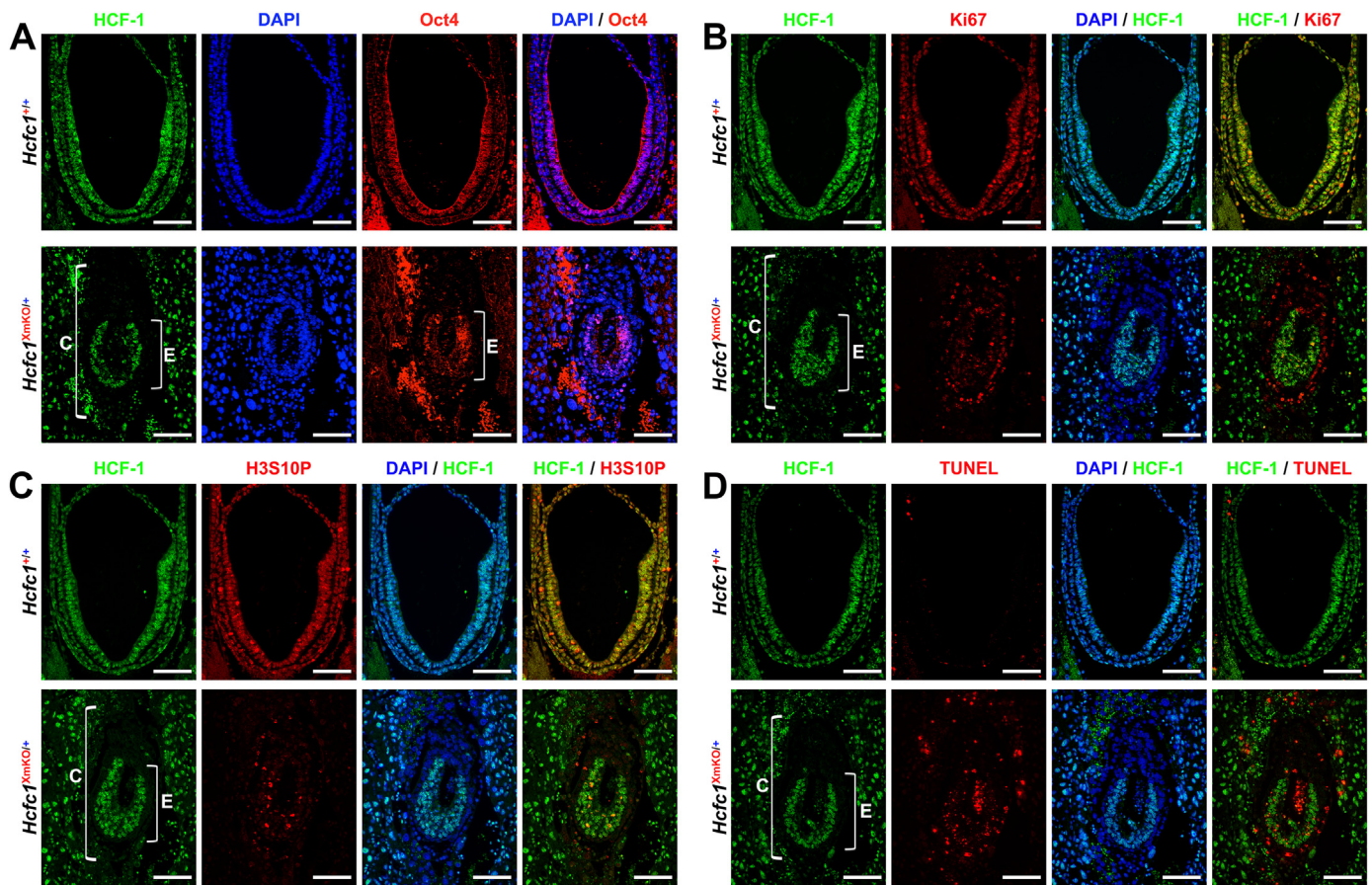


Fig. 3. A maternally inherited *Hcfc1*⁺ allele is required very early in development. Immunofluorescence analysis of E7.5 *Hcfc1*^{+/+} and *Hcfc1*^{XmKO/+} embryos obtained from the mating of *Sox2Cre*^{tg}; *Hcfc1*^{epiKO/+} female and *Hcfc1*^{+/-} male mice (Cross 1 of Table 3). All sections were stained with DAPI (blue) and anti-HCF-1 antibody (green) together with antibodies against (A) the epiblast-cell marker Oct4 (red), (B) the cell-proliferation marker Ki67 (red), or (C) the interphase and M-phase marker H3S10P (red). (D) Sections were stained with TUNEL (red) together with anti-HCF-1 antibody (green) and DAPI (blue). TUNEL-positive apoptotic cells are shown in red. C, conceptus; E, epiblast. Scale bar: 100 μm.

heterozygous *Hcfc1*^{XmKO/+} pups were non-existent and embryos were highly abnormal (column 4; see below). These results indicate that the maternal Xm *Hcfc1*⁺ allele is required in extraembryonic tissue and/or before the epiblast stage of embryonic development.

To explore the nature of the lethality generated by the maternal *Hcfc1*^{XmKO} allele, we immunostained paraffin sections of embryos obtained from Cross 1 at E7.5 as shown in Fig. 3. For this analysis, we used Oct4 immunofluorescence to distinguish embryonic (Oct4 positive) and extraembryonic (Oct4-negative) tissues (Fig. 3A). Wild-type embryos (Table 3, columns 1 and 3) revealed HCF-1 staining in both embryonic and extraembryonic (visceral endoderm) tissues (Fig. 3A–D, top panels). In wild-type embryos there was also marked staining for the broad cell-proliferation marker Ki67 (Scholzen and Gerdes, 2000) (Fig. 3B) and the interphase and mitotic marker histone H3 phosphorylated at serine 10 (H3S10P) (Prigent and Dimitrov, 2003) (Fig. 3C), thus displaying an active proliferation phenotype. Furthermore, TUNEL assays revealed little apoptosis (Fig. 3D).

In contrast, the highly abnormal *Hcfc1*^{XmKO/+} female embryos (Table 3, column 4), with Xm *Hcfc1*^{XmKO} and Xp *Hcfc1*⁺ alleles, were significantly smaller in size (Fig. 3A–D) than their wild-type littermate embryos. Consistent with maternal *Hcfc1*^{XmKO} inheritance, HCF-1 immunostaining revealed an absence of HCF-1 in the extraembryonic region (Fig. 3A–D). The cells in the abnormal epiblast region (i.e., Oct4 positive; Fig. 3A bottom panel), however, were essentially all HCF-1 positive (Fig. 3A–D), which must be owing to an active wild-type paternal Xp *Hcfc1*⁺ allele.

Nevertheless, although HCF-1 positive, these abnormal embryos displayed a significant reduction in Ki67 and H3S10P labeling and a high proportion of apoptotic cells when compared to control embryos (Fig. 3B–D). These results are most easily explained if HCF-1 function is essential for proper extraembryonic development and that thus, in its absence, the extraembryonic tissue cannot support proper embryonic development.

3.5. An *Hcfc1*^{cKO} allele on the paternally inherited X in *Hcfc1*^{+/-XpKO} heterozygotes is viable

Cross 2 tests the phenotype of *Hcfc1* inactivation on the paternally inherited Xp chromosome at the onset of development. The outcome of Cross 2 (*Sox2Cre*^{tg}; *Hcfc1*^{epiKO/+} × *Hcfc1*^{lox/Y}) is influenced by the presence of the *Sox2Cre*^{tg} allele in the mothers, because the *Sox2Cre*^{tg} allele is expressed in the female germ-line and the Cre recombinase enzyme thus synthesized in the oocyte is maternally inherited in the zygote irrespective of the segregation of the autosomal *Sox2Cre* transgene (Hayashi et al., 2003; Vincent and Robertson, 2003). Such maternally inherited Cre recombinase will result in efficient loxP-site induced recombination throughout the embryonic and extraembryonic derivatives of the early embryo (Hayashi et al., 2003; Vincent and Robertson, 2003). Thus, in this cross, the Xp *Hcfc1*^{lox} allele is expected to undergo efficient cKO deletion following fertilization. Consistent with this expectation, in this cross, the *Hcfc1*^{Xplox} allele did not survive irrespective of whether the *Sox2Cre*^{tg} transgene was inherited or not, indicating that the loxP to cKO conversion was 100% efficient and thus readily

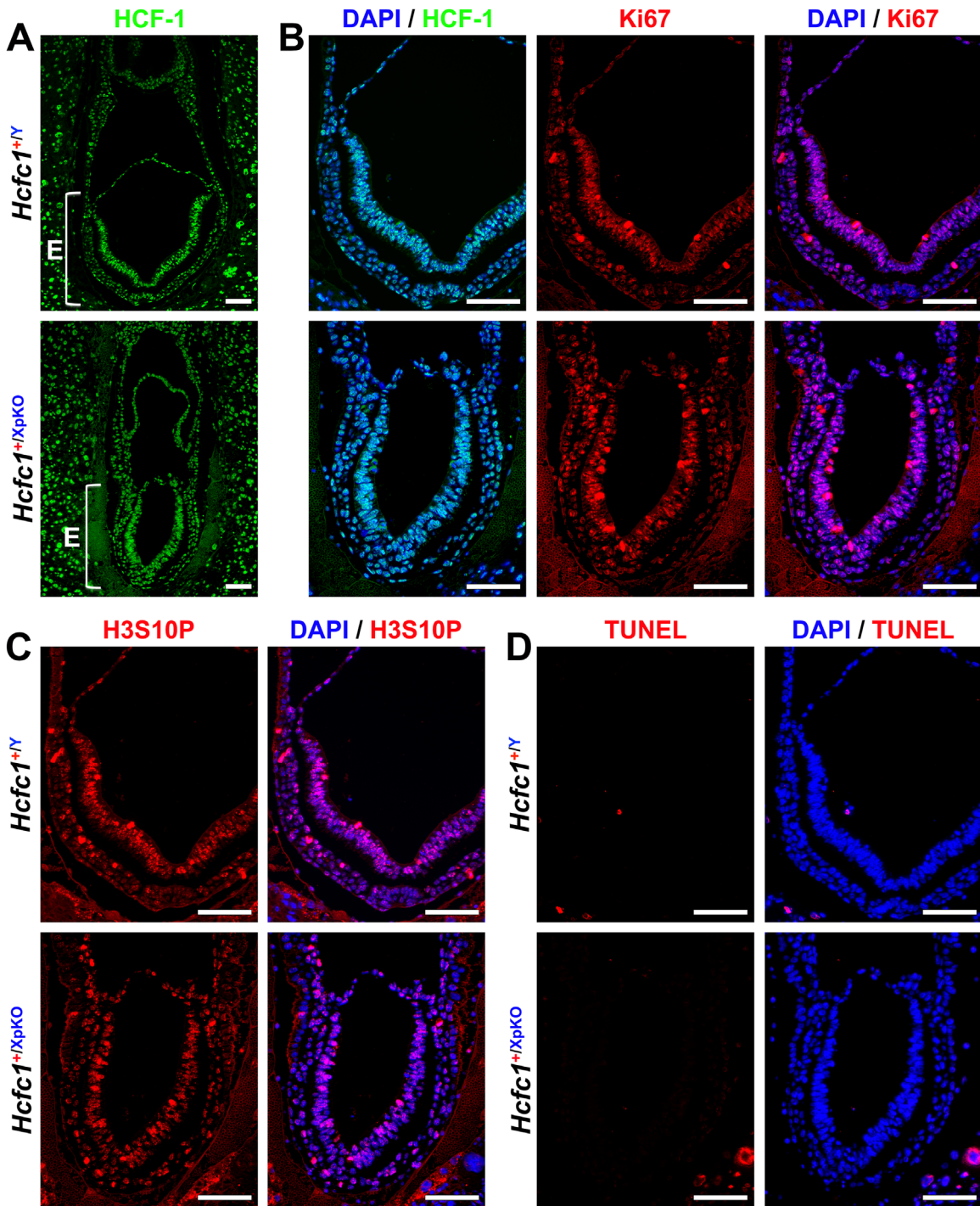


Fig. 4. Generation of *Hcfc1*^{XpKO} allele on the paternally inherited X chromosome is tolerated. Immunofluorescence analysis of E7.5 *Hcfc1*^{+Y} and *Hcfc1*^{+XpKO} embryos obtained from the mating of *Sox2Cre*^{tg}; *Hcfc1*^{epiKO/+} female and *Hcfc1*^{lox/Y} male mice (Cross 2 of Table 3). (A) Sections were stained with DAPI (blue) and anti-HCF-1 antibody (green). (B) High magnification view of the sections shown in (A) together with immunostaining against the cell-proliferation marker Ki67 (red). (C) Sections were stained with the interphase and M-phase marker H3S10P (red). (D) Sections were stained with TUNEL (red) and DAPI (blue). E, epiblast. Scale bar: 100 μ m.

supported by the maternally inherited Cre enzyme.

Interestingly, although as expected from the results of Cross 1 described above we did not obtain male or female embryos with the maternally inherited *Hcfc1*^{XmKO} allele (Table 3, columns 2 and 6; p -value 2.3×10^{-9}), we did obtain, albeit in somewhat lower numbers, normal female embryos and pups carrying the paternally inherited *Hcfc1*^{XpKO} allele (column 5, p -value relative to wild-type *Hcfc1*^{+Y} = 0.15). As shown in Fig. 4, however, the E7.5 embryos were smaller, indicating a transitory developmental retardation (see also below). Comparative HCF-1 immunostaining of

littermate wild-type and heterozygous *Hcfc1*^{+XpKO} female embryos at E7.5 revealed HCF-1 throughout the embryonic and extraembryonic tissue (Fig. 4). Additionally, labeling for Ki67 and H3S10P (Fig. 4B and C) demonstrated active proliferation and TUNEL staining (Fig. 4D) demonstrated little cell death throughout, as in wild-type. Thus, inheritance of the Xm *Hcfc1*^{XmKO} allele is lethal but very early *Hcfc1*^{XpKO} allele generation on the Xp chromosome is tolerated. Together, the results of Crosses 1 and 2 suggest that *Hcfc1*-gene function is essential for extraembryonic and/or very early embryonic development. Similar parent-of-origin

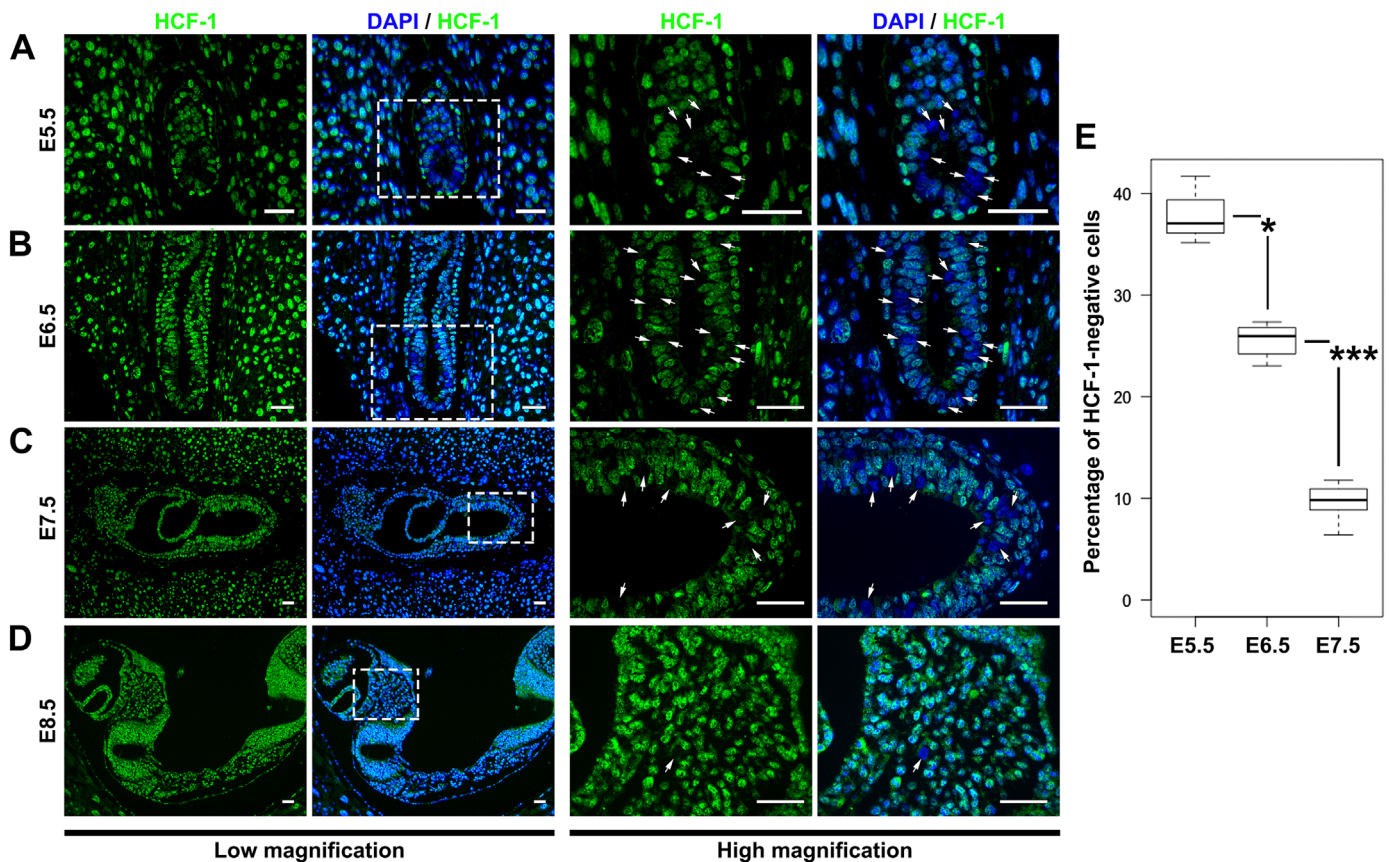


Fig. 5. *Sox2Cre^{tg}; Hcf1^{epiKO/+}* embryos exhibit progressive loss of HCF-1-negative cells from E5.5 to E8.5. Immunofluorescence analysis of HCF-1 in paraffin-embedded sections of *Sox2Cre^{tg}; Hcf1^{epiKO/+}* heterozygous female embryos at (A) E5.5, (B) E6.5, (C) E7.5, and (D) E8.5. Nuclei were stained with DAPI (blue) and HCF-1 antibody (green). The boxed regions at E5.5, E6.5, E7.5, and E8.5 are shown at higher magnification in subsequent panels. The arrows indicate HCF-1-negative DAPI-stained nuclei. (E) Percentage of HCF-1-negative cells from E5.5 to E7.5 ($n=3$ for E5.5, $n=8$ for E6.5, and $n=8$ for E7.5). (* p -value < 0.05, *** p -value < 0.001). Scale bar: 50 μ m.

effects on extraembryonic development have been observed previously for essential X-linked genes (Longo et al., 2002; O'Donnell et al., 2004).

Because an *Hcf1^{CKO}* allele could not be transmitted through the male nor female germ line, this *Hcf1^{CKO}* allele cannot be maintained by germ-line transmission.

3.6. *Hcf1^{epiKO}* allele initially resides on the female active or inactive X

As aforementioned (see Fig. 1C and Table 2), the *Hcf1^{lox}* to *Hcf1^{epiKO}* allele conversion is completely penetrant in *Hcf1^{epiKO/+}* females; thus, if *Hcf1^{epiKO/+}* females undergo random X-chromosome inactivation, cells should bear either one active *Hcf1⁺* or *Hcf1^{epiKO}* allele depending on the choice of inactivated X chromosome but not both. The lethality of *Hcf1^{epiKO/Y}* males thus raised the question as to expression of the *Hcf1⁺* and *Hcf1^{epiKO}* alleles in the cells of *Hcf1^{epiKO/+}* female mice – i.e., could cells whose active X chromosome carries the *Hcf1^{epiKO}* allele exist?

To address this question, as shown in Fig. 5A, we immunostained paraffin sections of *Sox2Cre^{tg}; Hcf1^{epiKO/+}* embryos at E5.5 at which point we know from their male siblings (Fig. 2) that they will have undergone Cre recombinase-induced *Hcf1^{epiKO}*-allele conversion. In these embryos, the epiblast was a mixture of 60–65% HCF-1-positive and 35–40% HCF-1-negative nuclei (Fig. 5A and E; arrows indicate HCF-1-negative nuclei). The number of HCF-1-negative nuclei was twofold higher in male E5.5 hemizygous *Hcf1^{epiKO/Y}* embryos (65–70%; Fig. 2) than in the female *Hcf1^{epiKO/+}* embryos (35–40%); this result can be explained if there is little to no a priori skewing of X-chromosome

inactivation such that roughly half the epiblast cells carry either the wild-type *Hcf1⁺* or mutant *Hcf1^{epiKO}* allele on the active X chromosome. This result is consistent with (i) effective *Hcf1^{epiKO}* allele generation at around E4.5 to E5.5 (Fig. 2; Hayashi et al., 2002), (ii) X-chromosome inactivation during the same period (Mak et al., 2004; McMahon et al., 1983; Rastan, 1982), and (iii) relatively rapid depletion by HCF-1 turnover or dilution in proliferating cells.

3.7. HCF-1-positive cells compensate for and replace HCF-1-negative cells during *Hcf1^{epiKO/+}* female embryonic development

The embryonic lethality of *Hcf1^{epiKO/Y}* males (Table 2) suggests that heterozygous *Hcf1^{epiKO/+}* female embryos that represent a mixture of HCF-1-positive and -negative cells (Fig. 5A) survive because cells positive for HCF-1 are able to compensate for those that are negative for HCF-1. Such compensation could be non-cell autonomous such that late stage embryos or adults possess both HCF-1-positive and -negative cells. Alternatively, *Hcf1* function could be required cell autonomously in which case HCF-1-positive cells must somehow replace HCF-1-negative cells. For example, *Hcf1* function may be required in specific tissues and only HCF-1-positive cells populate those tissues; alternatively *Hcf1* function may be universally required such that HCF-1-negative cells completely disappear.

To discriminate among these possibilities, we assayed the presence and absence of HCF-1-positive and -negative cells past E5.5. Fig. 5 shows the results of the analysis of stages E6.5 (Fig. 5B), E7.5 (Fig. 5C), and E8.5 (Fig. 5D), with quantitation shown in Fig. 5E for E5.5 through E7.5. Indeed, from E6.5 to E7.5, HCF-1-negative cells continued to persist (Fig. 5B and C, see white arrows) but

their levels progressively decreased to approximately 25% (E6.5) and 10% (E7.5) of the total embryonic cells (Fig. 5E), such that by E8.5 HCF-1-negative cells had essentially disappeared (Fig. 5D, see arrow) to a single evident HCF-1-negative cell. These results suggest that HCF-1 function is essential and cell autonomous, such that HCF-1-positive cells broadly and progressively replace and compensate for HCF-1-negative cells during a period of embryogenesis that encompasses gastrulation, a process key in the initiation of tissue differentiation.

The observed mixed population of HCF-1-positive and -negative cells early in embryogenesis followed by an eventual dominance of HCF-1-positive cells later in embryogenesis is most easily explained if cells carrying the *Hcfc1*⁺ allele on the active X chromosome are positively selected during *Hcfc1*^{epiKO/+} embryogenesis. To address this hypothesis directly, we employed an X chromosome marked with a

green fluorescent protein transgene called *XGFP* (Hadjantonakis et al., 2001, 1998); cells carrying the *XGFP*^{tg} transgene will immunostain for GFP only when the *XGFP* allele is active thus allowing the determination of which X chromosome is active. We crossed *Hcfc1*^{+ / Y} male mice carrying the *Sox2Cre*^{tg} and *XGFP*^{tg} transgenes with *Hcfc1*^{lox/lox} females. Female offspring will carry an Xp *XGFP*^{tg} chromosome linked to the wild-type *Hcfc1*⁺ allele, and either an *Hcfc1*^{lox} or – eventually – *Hcfc1*^{epiKO} allele on the Xm chromosome depending on the absence or presence of the *Sox2Cre*^{tg} transgene, respectively. In contrast, male offspring cannot carry the Xp *XGFP*^{tg} chromosome.

The results of this experiment are shown in Fig. 6, with GFP levels analyzed by whole-mount GFP immunostaining. As expected, the *Hcfc1*^{lox/Y} male embryos did not display specific GFP staining at any stage (Fig. 6A, D, and G). In contrast, both E6.5 *Hcfc1*^{lox/+} and *Hcfc1*^{epiKO/+} *XGFP*^{tg} embryos displayed a mottled

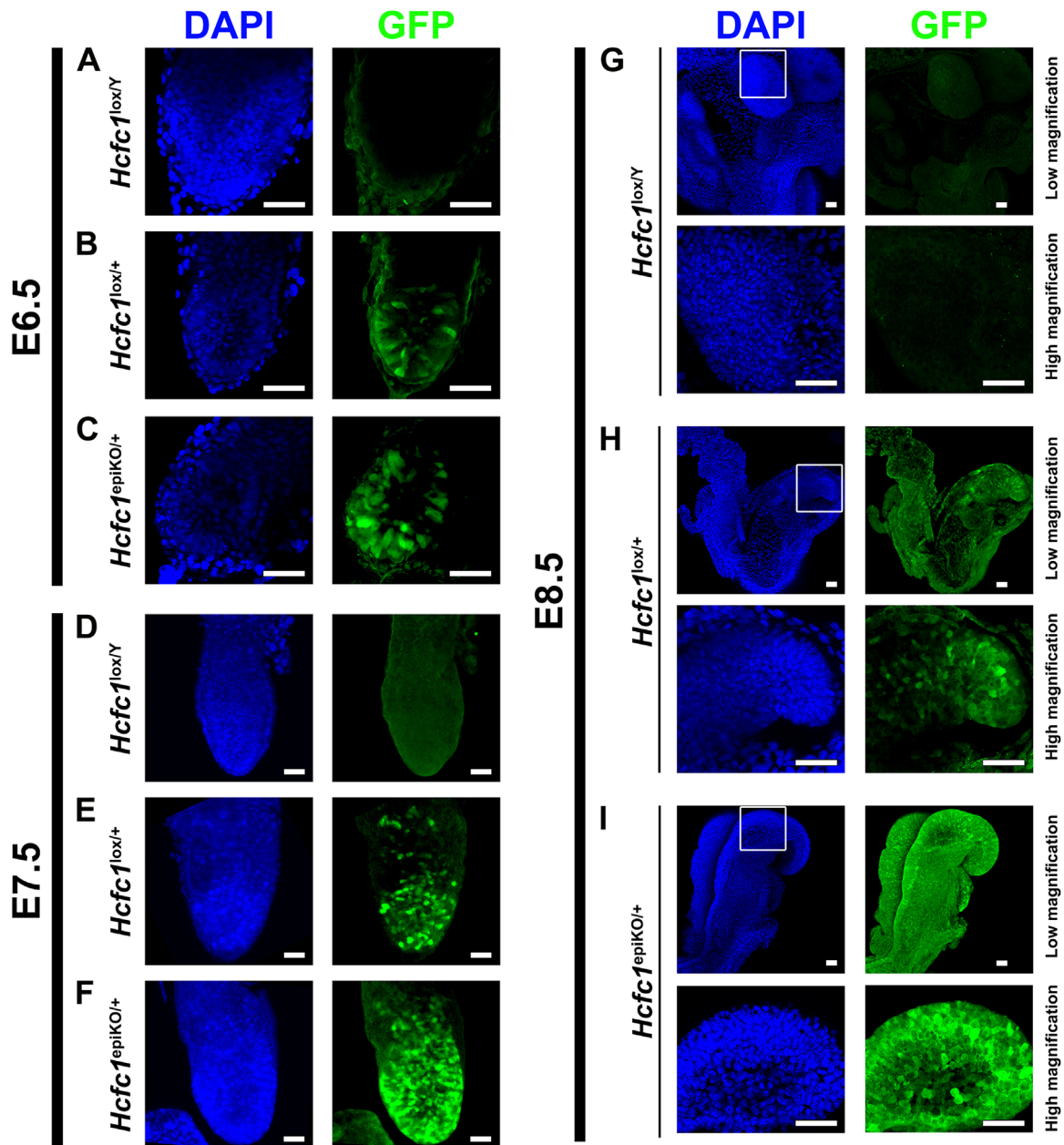


Fig. 6. *Hcfc1*^{epiKO/+}; *XGFP*^{tg} embryos exhibit progressive gain of *Hcfc1*⁺-linked X-chromosome expression from E6.5 to E8.5. Immunofluorescence analysis of embryos obtained from mating *Hcfc1*^{+ / Y} male mice carrying *Sox2Cre*^{tg} and *XGFP*^{tg} alleles with *Hcfc1*^{lox/lox} female mice. Female offspring carry the *XGFP*^{tg} transgene and the *Hcfc1*⁺ allele on the same chromosome, and *Hcfc1*^{lox} or *Hcfc1*^{epiKO} allele on the other. The progeny were collected at E6.5 (A–C), E7.5 (D–F), and E8.5 (G–I). Whole mount embryos were stained with DAPI (blue) and anti-GFP (green) antibodies. The boxed regions in (G) *Hcfc1*^{lox/Y}, (H) *Hcfc1*^{lox/+}; *XGFP*^{tg}, and (I) *Hcfc1*^{epiKO/+}; *XGFP*^{tg} embryos at E8.5 are shown at higher magnification in the panels in the row below. Scale bar: 25 μm.

GFP staining pattern (Fig. 6B and C) consistent with random inactivation of the *XGFP^{tg}* chromosome. In concordance with the disappearance of HCF-1-negative cells in *Hcfc1^{epiKO/+}* embryos, over the next two days of development, the percentage of GFP-positive cells (carrying the active wild-type *Hcfc1⁺* allele) increased such that, throughout the entire embryo, we failed to observe tissues with GFP-negative cells (compare Fig. 6E and F, and H and I). We also similarly assayed GFP – as well as HCF-1 – levels in the eye later in embryonic development (i.e., E14.5; Supplemental Fig. 6) and in early postnatal (P5) brain and liver (Supplemental Fig. 7) and similarly observed a broad, essentially universal, presence of GFP and HCF-1 in the *Hcfc1^{epiKO/+}*; *XGFP^{tg}* but not *Hcfc1^{lox/+}*; *XGFP^{tg}* mice.

These results suggest an early universal strong selection for the *Hcfc1⁺* allele on the active X chromosome (i.e., HCF-1-positive

cells) leading to 100% selection of cells carrying the *Hcfc1^{epiKO}*-allele on the inactive X-chromosome – a so-called complete secondary skewing of X-chromosome inactivation. This skewing by which HCF-1-positive cells compensate for HCF-1-negative cells is apparently effective: although *Hcfc1^{epiKO/+}* embryos are reduced in size and developmentally retarded between E6.5 and at least E8.5 (Supplemental Fig. 8A–C) – owing to an apparent subsequent acceleration in development and growth – this reduction is largely transient as, for example, E9.5 (Supplemental Fig. 4B) and E14.5 (Supplemental Fig. 8D) *Hcfc1^{lox/+}* and *Hcfc1^{epiKO/+}* embryos are of similar size. Combined with the high frequency of *Hcfc1^{epiKO/+}* heterozygous pup births (Table 2), the *Hcfc1^{epiKO/+}* developmental profile indicates that the replacement of HCF-1-negative cells by the HCF-1-positive ones in *Hcfc1^{epiKO/+}* embryos is highly effective to maintain viability.

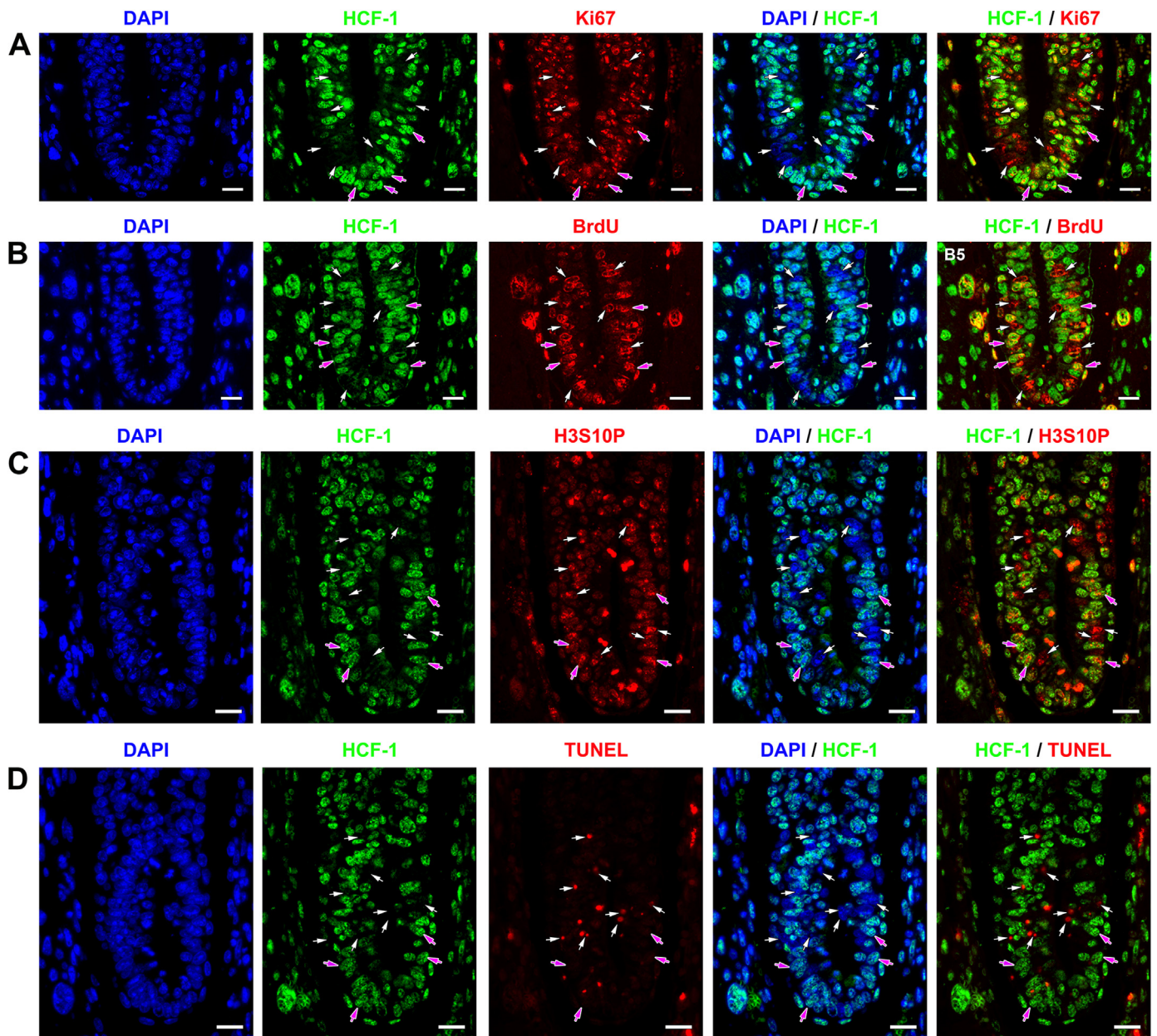


Fig. 7. HCF-1-negative cells can proliferate at E6.5. Immunofluorescence analysis of paraffin-embedded sections of *Sox2Cre^{tg}*; *Hcfc1^{epiKO/+}* heterozygous female embryos at E6.5. All sections were stained with DAPI (blue) and anti-HCF-1 antibody (green) together with antibodies against (A) the cell-proliferation marker Ki67 (red), (B) the S-phase marker BrdU following 6 h BrdU incorporation (red), or (C) the interphase and M-phase marker H3S10P (red). (D) TUNEL assay was performed on sections co-stained with DAPI (blue) and anti-HCF-1 antibody (green). TUNEL-positive apoptotic cells are shown in red. In A–D, the white arrows point to HCF-1-negative nuclei and magenta arrows point to a few HCF-1-positive nuclei. Scale bar: 50 μ m.

3.8. HCF-1-negative cells proliferate in E6.5 embryos

Hcfc1 is implicated in cell proliferation (Goto et al., 1997; Julien and Herr, 2003). Thus, the presence in Fig. 5 of large numbers of HCF-1-negative cells in E6.5 embryos one to two days after *Hcfc1*^{lox} to *Hcfc1*^{epiKO} conversion was surprising. We hypothesized that at E6.5 after *Hcfc1*^{lox} to *Hcfc1*^{epiKO} conversion HCF-1-negative embryonic cells might still proliferate. To test this hypothesis we co-stained E6.5 *Hcfc1*^{epiKO/+} embryos for HCF-1 and three cell-cycle markers: Ki67, the S-phase marker BrdU, and H3S10P. As shown in Fig. 7 and quantitated in Fig. 9A (see also Supplemental Table 3), E6.5 HCF-1-negative cells (white arrows) are frequently positive for Ki67 (Fig. 7A), BrdU incorporation (Fig. 7B), and H3S10P (Fig. 7C), indicating that indeed HCF-1-negative cells continue to proliferate.

Nevertheless, eventually the HCF-1-negative cells disappear. Consistent with this observation, (i) at E7.5 we observe many HCF-1-negative – but not HCF-1-positive – cells missing the Ki67 cell-proliferation marker (Figs. 8A and 9B), and (ii), as evidenced by TUNEL assays (Figs. 7D and 8B and quantitated in Fig. 9), E6.5 and E7.5 HCF-1-negative – but not HCF-1-positive – cells undergo apoptosis. Thus continued proliferation of HCF-1-negative cells appears to lead to cell-cycle exit and eventual apoptosis and disappearance.

3.9. HCF-1 is crucial for proliferation during liver regeneration

The requirement for HCF-1 in mammalian cell proliferation has been established in tissue culture cells, but not in an in vivo physiological context. The continued proliferation of HCF-1-deficient cells observed here during early embryogenesis does not reveal an immediate essential HCF-1 function in embryonic cell proliferation. We thus also addressed a role for HCF-1 in cell

proliferation in a non-embryonic context, by taking advantage of the high regenerative potential of the mammalian liver. After two-thirds partial hepatectomy (PH), remaining resting hepatocytes rapidly and synchronously re-enter the cell-division cycle to regenerate the liver mass within one to two weeks (Fausto et al., 2006; Michalopoulos and DeFrances, 1997; Taub, 2004). We utilized this regenerative ability of the liver to study HCF-1 function in de novo cell-proliferation entry and progression by resting cells.

For this purpose, we induced hepatocyte-specific deletion of the *Hcfc1*^{lox} allele (called *Hcfc1*^{hepKO}, see Table 1) by tamoxifen activation of an Albumin-Cre (*Alb-Cre-ERT2*^{tg}) allele (Schuler et al., 2004) in 10–14 week-old *Alb-Cre-ERT2*^{tg}; *Hcfc1*^{lox/Y} males and *Alb-Cre-ERT2*^{tg}; *Hcfc1*^{lox/+} females, thus generating knockout *Hcfc1*^{hepKO/Y} and heterozygous *Hcfc1*^{hepKO/+} hepatocytes, respectively. Prior to tamoxifen treatment, all *Alb-Cre-ERT2*^{tg}; *Hcfc1*^{lox/+} hepatocytes and non-hepatocytes – identified as hepatocyte nuclear factor α (HNF4 α)-positive (green arrows in Fig. 10B) and -negative (mauve arrows) cells, respectively – are positive for HCF-1 (Fig. 10A and B), indicating that the Cre-ERT2 recombinase activity is strongly tamoxifen dependent. Post-tamoxifen treatment, immunoblot analysis of *Alb-Cre-ERT2*^{tg}; *Hcfc1*^{lox/Y} males demonstrated progressive and significant loss of HCF-1 protein (Supplemental Fig. 9), consistent with activated *Alb-Cre-ERT2*^{tg}-induced *Hcfc1*^{lox} to *Hcfc1*^{hepKO} allele conversion. Since the expression of *Alb-Cre-ERT2*^{tg} transgene is hepatocyte-specific, presence of some HCF-1 protein could be still seen at the end of fifth day owing to non-hepatocytes that are not affected.

In, however, *Alb-Cre-ERT2*^{tg}; *Hcfc1*^{lox/+} females seven days post-tamoxifen treatment (Fig. 10C and D), whereas smaller HNF4 α -negative non-hepatocyte liver cell types remain HCF-1 positive (mauve arrow, Fig. 10D), patches of HNF4 α -positive hepatocytes either HCF-1-positive (green arrow, Fig. 10D) or HCF-1-negative (white arrow and dashed line ovals, Fig. 10D) appear. The HCF-1-negative clusters

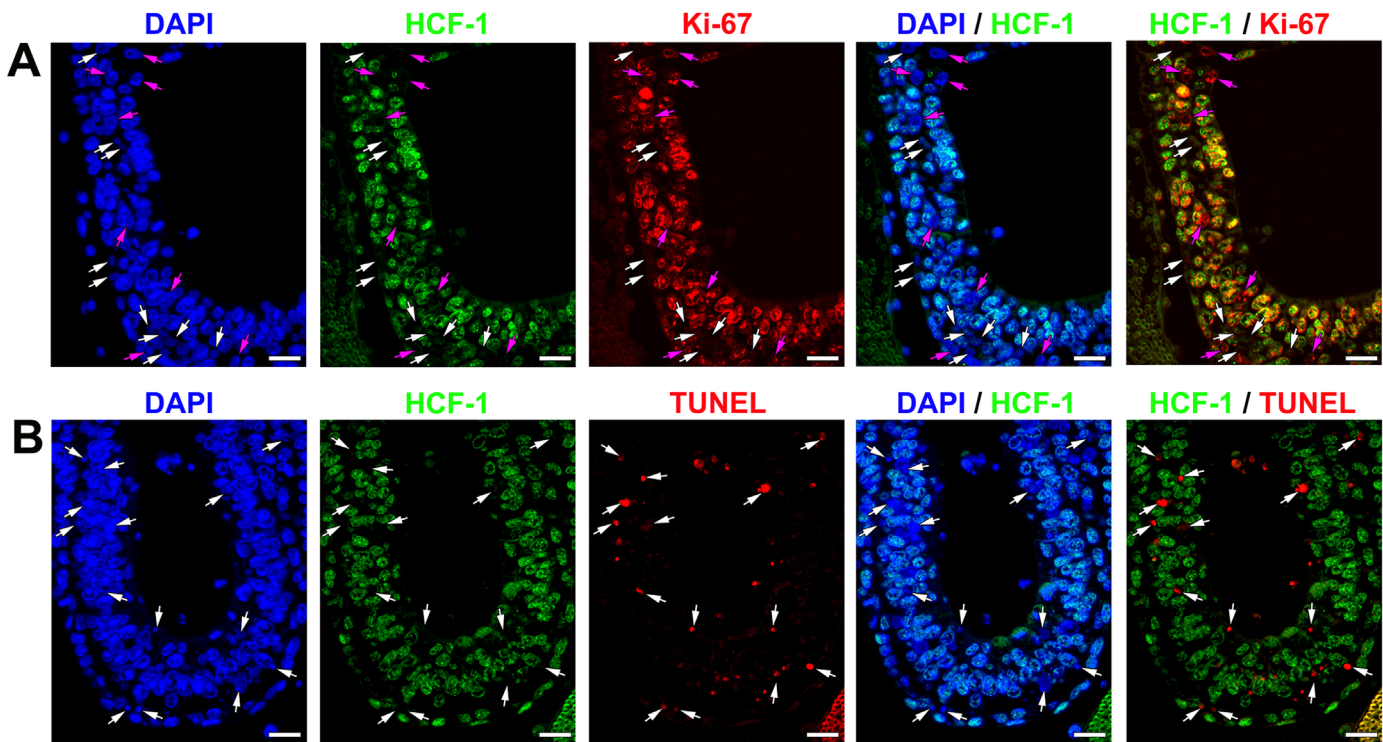


Fig. 8. At E7.5, *Hcfc1*^{epiKO/+} HCF-1-negative cells display divergent phenotypes – proliferative, non-proliferative or apoptotic. Immunofluorescence analysis of paraffin-embedded sections of *Sox2Cre*^{tg}; *Hcfc1*^{epiKO/+} heterozygous female embryos at E7.5. (A) The section was stained with DAPI (blue), anti-HCF-1 (green), and anti-Ki67 (red) antibodies. The white arrows identify HCF-1-negative nuclei that are Ki67 negative. The magenta arrows identify HCF-1-negative nuclei that are Ki67 positive. (B) TUNEL assay was performed on a section co-stained with DAPI (blue) and anti-HCF-1 antibody (green). TUNEL-positive apoptotic cells are shown in red. The white arrows identify HCF-1-negative nuclei that are TUNEL positive. Scale bar: 50 μ m.

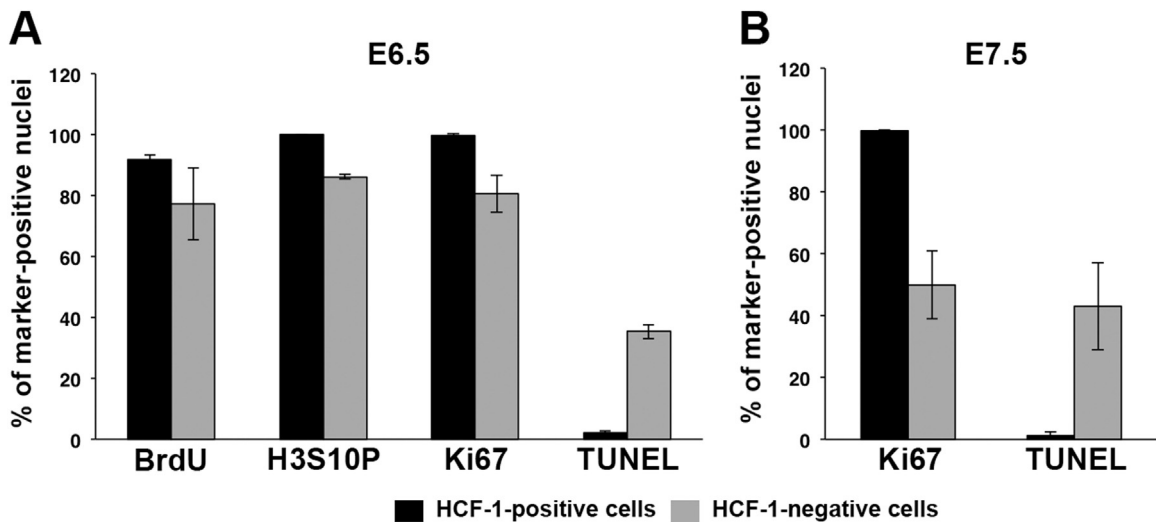


Fig. 9. Transient proliferation of HCF-1-negative cells is eventually followed by apoptosis. Quantification of the data presented in Figs. 7 and 8. (A) Graph showing the percentages of HCF-1-positive (black) and HCF-1-negative (gray) cells positive for labeling for BrdU, H3S10P, Ki67 or TUNEL in sections of *Sox2Cre^{tg}; Hcfc1^{epiKO/+}* heterozygous female embryos at E6.5. The difference between percentages of HCF-1-positive and HCF-1-negative cells also positive for BrdU (p -value 0.08) was not significant ($n=4$). The differences between percentages of HCF-1-positive and HCF-1-negative cells also positive for H3S10P (p -value 0.02; $n=2$), Ki67 (p -value 0.002; $n=5$), and TUNEL (p -value 3.1×10^{-5} ; $n=4$) were significant. (B) Graph showing the percentages of HCF-1-positive (black) and HCF-1-negative (gray) cells positive for labeling for Ki67 or TUNEL in sections of *Sox2Cre^{tg}; Hcfc1^{epiKO/+}* heterozygous female embryos at E7.5. The difference between percentages of HCF-1-positive and HCF-1-negative cells also positive for Ki67 (p -value 5×10^{-4} ; $n=5$) and TUNEL (p -value 7×10^{-4} ; $n=6$) were highly significant.

are probably owing to clones of cells descendent from single progenitor cells in which the *Hcfc1^{lox}* allele was on the active X chromosome and the HCF-1-positive clusters are probably owing to

clones of cells descendent from single progenitor cells in which the *Hcfc1^{lox}* allele was on the inactive X chromosome.

Seven days post-tamoxifen treatment of *Alb-Cre-ERT2^{tg}*;

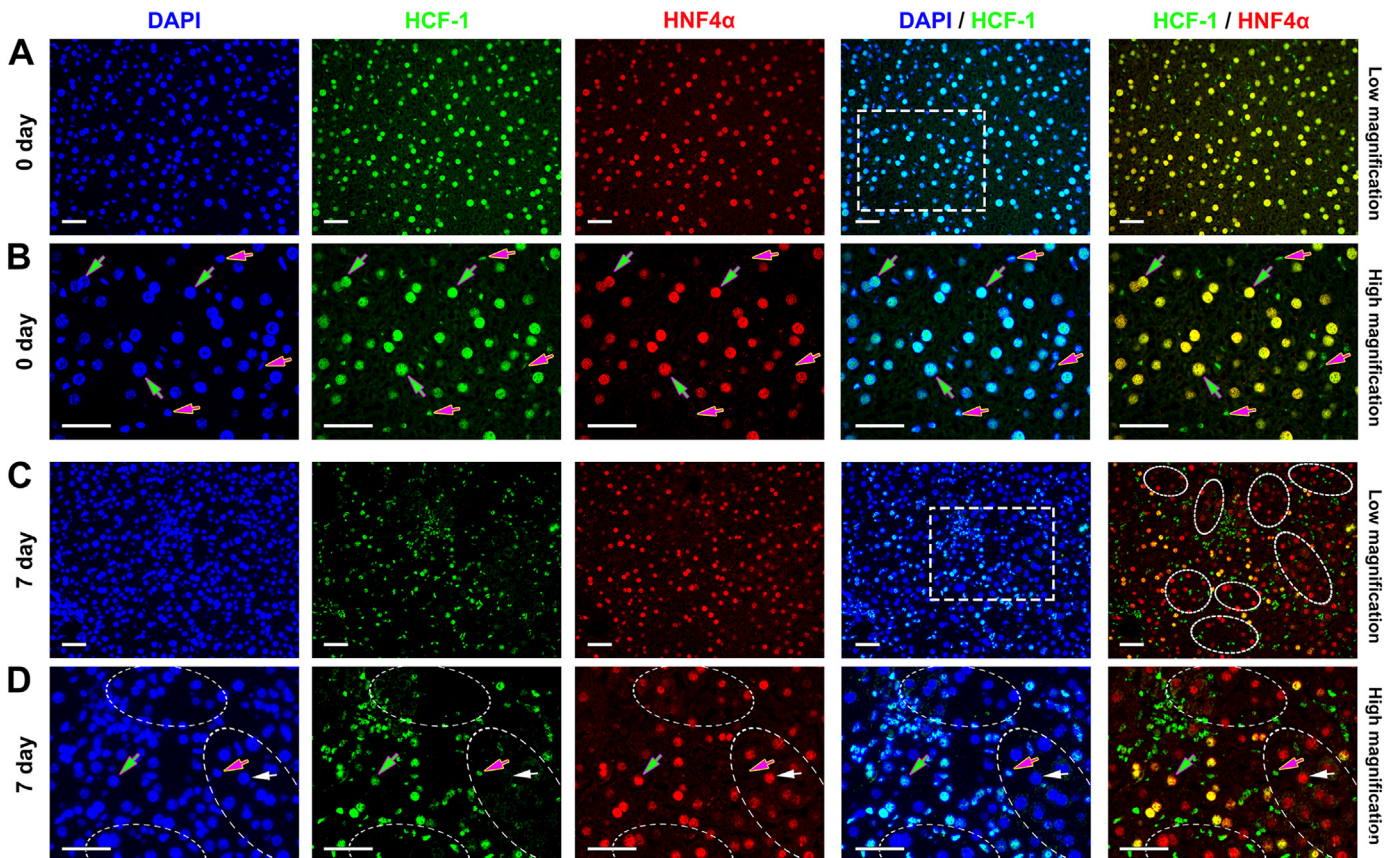


Fig. 10. Hepatocyte-specific *Hcfc1^{hepKO}}* allele generation in *Alb-Cre-ERT2^{tg}; Hcfc1^{lox/+}* mice. Immunofluorescence analysis of HCF-1 in paraffin-embedded liver sections from (A and B) *Alb-Cre-ERT2^{tg}; Hcfc1^{lox/+}* control and (C and D) 7-day post-tamoxifen treatment *Alb-Cre-ERT2^{tg}; Hcfc1^{hepKO/+}* 10-week old mice. The sections were stained with DAPI (blue), and anti-HCF-1 (green) and hepatocyte-specific anti-HNF4 α (red) antibodies. The boxed regions in A and C mark the regions shown at higher magnification in the panels B and D, respectively. Tamoxifen induction generates the *Hcfc1^{hepKO}}* allele as demonstrated by the 7-day post-treatment loss of HCF-1 protein in specific clusters (broken oval lines) of hepatocytes (C and D). Green arrows point to HCF-1-positive and HNF4 α -positive hepatocytes; purple arrows point to HCF-1-positive and HNF4 α -negative non-hepatocytes; and white arrow points to an HCF-1-negative and HNF4 α -positive hepatocyte. Scale bar: 50 μ m.

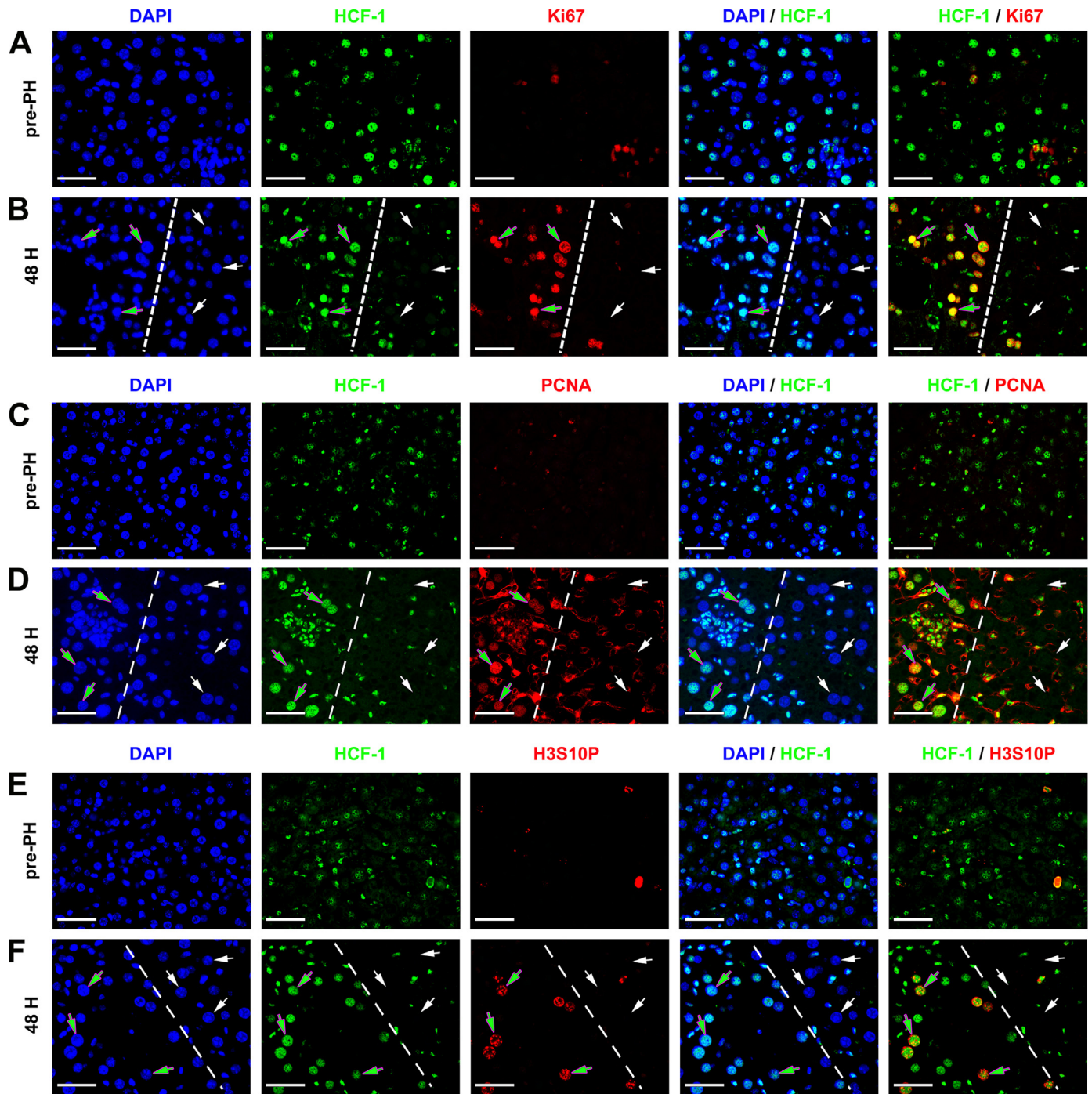


Fig. 11. Hepatocytes lacking HCF-1 fail cell-division cycle entry upon partial hepatectomy. Immunofluorescence analysis of cell-cycle progression markers of 10-week old *Alb-Cre-ERT2^{tg}; Hcfc1^{hepKO/+}* heterozygous female mice 7 days post-tamoxifen treatment before and 48 h after being subjected to 70% PH. The paraffin-embedded sections of livers before (A, C, and E) and 48 h after (B, D, and F) PH were stained with DAPI (blue), anti-HCF-1 (green), and one of three cell-proliferation markers shown in red: (A and B) Ki67, (C and D) PCNA, and (E and F) H3S10P. The broken lines in B, D, and F separate the HCF-1-positive from HCF-1-negative hepatocytes. The green arrows point to DAPI-, HCF-1- and cell-proliferation marker-positive hepatocytes, and the white arrows point to DAPI-positive, HCF-1-negative and cell-proliferation marker-negative hepatocytes. Scale bar: 50 μm .

Hcfc1^{lox/+} mice, we performed PH and analyzed the liver tissue 48 h later – at which point hepatocytes are actively passing through the cell-division cycle – for (i) Ki-67 (Fig. 11B), (ii) the S-phase marker Proliferating Cell Nuclear Antigen (PCNA) (Fig. 11D), which displays evident S-phase nuclear staining (Kelman, 1997), and (iii) H3S10P (Fig. 11F). Prior to PH, few if any tamoxifen-induced *Hcfc1^{hepKO/+}* hepatocytes were positive for any of these three cell-proliferation markers (Fig. 11A, C, and E); 48 h post-PH, however, many cells were positive for these three

markers (Fig. 11B, D, and F) but only in the patches of HCF-1-positive hepatocytes (green arrows) – hepatocytes lacking HCF-1 (white arrows) were negative for the three cell cycle markers (see also Supplemental Fig. 10), indicating that HCF-1 is required for proper hepatocyte proliferation during liver regeneration and thus important for cell-cycle re-entry by these resting cells. Quantitative analysis of the results shown in Fig. 12 (see also Supplemental Table 4) reinforces this conclusion.

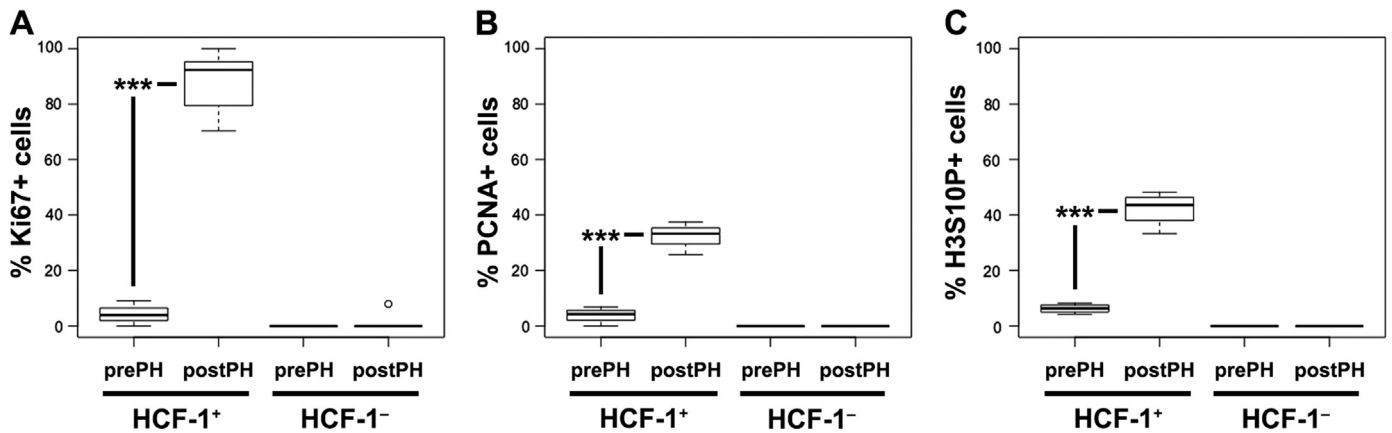


Fig. 12. Only HCF-1-positive cells enter into cell-division cycle upon partial hepatectomy. Quantification of the data presented in Fig. 11. Boxplots showing the percentage of HCF-1-positive (HCF-1⁺) and HCF-1-negative (HCF-1⁻) cells positive for labeling for (A) Ki67 ($n=3$ prePH; $n=5$ postPH) (p -value 1.9×10^{-5}), (B) PCNA ($n=4$ prePH; $n=3$ postPH) (p -value 6.6×10^{-3}), and (C) H3S10P ($n=4$ prePH; $n=4$ postPH) (p -value 9.0×10^{-4}) in sections of *Alb-Cre-ERT2^{tg}; Hcf1^{hepKO/+}* heterozygous female mice 7 days post-tamoxifen treatment before (prePH) and 48 h after (postPH) being subjected to 70% PH.

4. Discussion

We have generated a silent allele of the mouse *Hcf1* gene, called *Hcf1^{lox}*, that can be conditionally deleted with Cre recombinase. We take advantage of the broad expression and X-chromosome linkage of the *Hcf1* gene to study its role in embryonic and extraembryonic development, and adult tissue regeneration. An unexpected by-product of the X chromosome linkage of the *Hcf1* gene and the cell-autonomous requirement for HCF-1 in early embryonic-cell viability is the ability to genetically address the sensitivity of the early post-implantation embryo to major cell loss.

4.1. HCF-1 has extensive roles in cell proliferation

Our studies show that HCF-1 is important for both embryonic and extraembryonic mammalian development and illuminate its role in cell proliferation in two very different contexts: the post-implantation embryo and the adult regenerating liver. Significantly, these two contexts differ in the status of the cells in which HCF-1 is being depleted – in the embryonic cells HCF-1 is being depleted in proliferating cells whereas in the adult liver HCF-1 is being depleted in resting cells – and the effects differ. In the embryonic cells, although eventually having an effect, depletion of HCF-1 does not have an apparent immediate cell-proliferation arrest effect. This phenotype is reminiscent of the temperature-sensitive tsBN67 hamster cell line, in which cells continue to proliferate after shift to the non-permissive temperature (Goto et al., 1997).

In the case of the *Hcf1^{epiKO/+}* embryos, the delay in loss of HCF-1-negative cells may be owing to a period post *Hcf1^{epiKO}* induction in which, as examples, (i) it takes time for levels of HCF-1 (an abundant and stable protein; (Wilson et al., 1995; Wysocka et al., 2001)) to fall below the amount necessary to support cell proliferation (a level not being easily detected by our immunofluorescence analyses), (ii) loss of HCF-1 transcriptional regulatory function does not have an immediate effect on transcription of its regulatory targets (e.g., it could activate histone modifications that are maintained for some cell generations via an HCF-1-independent mechanism), or (iii) HCF-1 is not required for cell proliferation at the time of epiblast-specific inactivation.

Vis-à-vis the latter example, the ability of E6.5 HCF-1-negative cells to proliferate may be related to the rapid proliferation status of these cells where negative regulators of the cell-division cycle such as the pRb-related pocket protein family are apparently inactive (reviewed in Ciemerych and Sicinski (2005)). Indeed, inhibition of pRb-related pocket protein family function can

suppress the need for HCF-1 function in cell proliferation (Reilly et al., 2002) – E6.5 cells may represent such cells with suppressed pRb-related pocket protein family function.

In contrast, the essentially complete sensitivity of hepatocyte proliferation to HCF-1 depletion upon PH-induced liver regeneration may be explained by the fact that, in the liver regeneration protocol, it is possible to deplete resting hepatocytes over seven days before challenging them to proliferate de novo and HCF-1 is essential for de novo hepatocyte proliferation where the pRb-related pocket protein family is likely active.

4.2. HCF-1 plays early roles in embryonic cell proliferation

The generation of the epiblast-specific *Hcf1^{epiKO}* allele with the *Sox2Cre* transgene permits the study of HCF-1 function at an early stage of embryonic development – around E5.5 and beyond. Furthermore, as shown in Table 3, we did not observe any embryos that would have lacked HCF-1 from conception (i.e., *Hcf1^{XmKO/Y}* and *Hcf1^{XmKO/XpKO}* embryos), suggesting that HCF-1 plays a role in cell proliferation even before implantation. Consistent with this hypothesis, HCF-1 plays a positive role in embryonic stem-cell proliferation (Dejosez et al., 2010).

Even if only required after E7.5, few cell proliferation genes are required so early in development (Ciemerych and Sicinski, 2005). This very early requirement for *Hcf1* function could be because in vertebrates it is a member of a small gene family consisting of only two genes – *Hcf1* and the much smaller HCF-2-encoding *Hcf2* (Johnson et al., 1999) gene – such that there is little possibility for redundant gene functions. Additionally, HCF-1 associates with large numbers of transcriptional start sites in both embryonic-stem cells (743) and transformed HeLa cells (5400) (Dejosez et al., 2010; Michaud et al., 2013). Such potentially broad involvement in transcriptional regulation could explain an early essential role for HCF-1 in embryogenesis.

4.3. Development of the mouse post-implantation embryo is highly resistant to cell loss

Animal development involves cell proliferation in which cells become increasingly committed to particular developmental or differentiation pathways. The timing of such commitment and its sensitivity to perturbation varies among species. For example, in the deterministic development of the *Caenorhabditis elegans* worm embryo, differentiation commitment occurs during the first cell divisions and embryonic development is exquisitely sensitive to individual cell loss (Sulston et al., 1983). By contrast, early mammalian embryonic development is much less deterministic and

there is considerable plasticity in cell differentiation commitment, particularly prior to implantation (Martinez Arias et al., 2013). For example, embryonic cell-depletion experiments pre-implantation – either micromanipulation to remove one or two cells from two-to-four cell embryos (Power and Tam, 1993; Rands, 1986) or pharmacological intervention of 16–32 cell morula-stage embryos (Tam, 1988) – have shown eventual normal development post cell depletion.

Post-implantation, however – for example, during gastrulation which occurs at E6.5 to E7.5 – there is a rapid determination of cell differentiation pathways (e.g., the three germ layers). This progressive determination means that, as development progresses, cells will have followed a greater number of differentiation pathways and functional replacement to compensate for cell loss may become more difficult. Nevertheless, one study has shown that treatment of embryos at E6.5 to E7.0 with the cytotoxic drug mitomycin C can lead to a rapid 85% reduction in cell number and, in response, to an accelerated cell proliferation response, such that embryos recover in size and developmental stage by approximately E10.5 (Snow and Tam, 1979).

Here, by virtue of (i) an early embryonic cell-proliferation requirement for HCF-1 function, (ii) the X-chromosome linkage of the *Hcfc1* gene, and (iii) the creation of a Cre-inducible cKO *Hcfc1*^{lox} allele, we have probed through genetic manipulation, rather than pharmacological intervention, the resistance of the post-implantation mouse embryo to progressive cell loss beginning before and ending after gastrulation. In this case, although the lethality of *Hcfc1*^{epiKO/Y} male embryos would suggest otherwise, the progressive loss of HCF-1-negative cells in *Hcfc1*^{epiKO/+} female heterozygotes may be owing to cell competition, whereby HCF-1-negative cells are not inherently unable to proliferate but instead they are out-competed by the HCF-1-positive cells. Whether by a competitive or a non-competitive mechanism, this genetically engineered post-implantation loss of HCF-1-negative cells had little effect on developmental success even as the embryos underwent gastrulation, a critical phase of development. In this case, survival may be aided by the extensive salt and pepper pattern of HCF-1 loss such that all parts of the embryo have plenty of HCF-1-positive cells with which to compensate for cells lacking HCF-1. Whatever the case, our results show that mammalian embryonic plasticity permits the survival of female embryos heterozygous for an X-linked embryonic lethal allele.

Competing interest statement

The authors declare that they have no competing interests.

Author contributions

The experiments were conceived and designed by S.M., T.-L.S., and W.H. The experiments were performed by S.M., T.-L.S., D.V., and F.L. S.M., T.-L.S., and W.H. analyzed the data. S.M. and W.H. wrote the paper. All authors participated in the discussion of the data and in production of the final version of the manuscript.

Acknowledgments

We thank D. Pinatel for technical assistance; C. Moret for help with tissue sectioning and staining; V. Praz for bioinformatics support; P. Chambon and D. Metzger for the *Alb-Cre-ERT2^{tg}* mice; A. Buil for help with statistical analyses; S. Bessonard and D. Constam for technical advice and discussions; the UNIL-CHUV

Mouse Metabolic Facility for the *EchoMRI* analyses; E. Heard and A. McMahon for discussions; and S. Bessonard, D. Constam, and N. Hernandez for critical readings of the manuscript. This research was supported by Swiss National Science Foundation grant 31003A_147104 and the University of Lausanne.

Appendix A. Supplementary material

Supplementary data associated with this article can be found in the online version at <http://dx.doi.org/10.1016/j.ydbio.2016.02.019>.

References

- Augui, S., Nora, E.P., Heard, E., 2011. Regulation of X-chromosome inactivation by the X-inactivation centre. *Nat. Rev. Genet.* 12, 429–442.
- Ciemerych, M.A., Sicinski, P., 2005. Cell cycle in mouse development. *Oncogene* 24, 2877–2898.
- Dejosez, M., Levine, S.S., Frampton, G.M., Whyte, W.A., Stratton, S.A., Barton, M.C., Gunaratne, P.H., Young, R.A., Zwaka, T.P., 2010. Ronin/Hcf-1 binds to a hyperconserved enhancer element and regulates genes involved in the growth of embryonic stem cells. *Genes Dev.* 24, 1479–1484.
- Fausto, N., Campbell, J.S., Riehle, K.J., 2006. Liver regeneration. *Hepatology* 43, S45–53.
- Frattini, A., Chatterjee, A., Faranda, S., Sacco, M.G., Villa, A., Herman, G.E., Vezzoni, P., 1996. The chromosome localization and the HCF repeats of the human host cell factor gene (HCF1) are conserved in the mouse homologue. *Genomics* 32, 277–280.
- Gohar, A.V., Mohammadi, A., 2009. A simple method for DNA extraction from formalin-fixed, paraffin embedded tissue blocks. *Protoc. Online*.
- Goto, H., Motomura, S., Wilson, A.C., Freiman, R.N., Nakabeppu, Y., Fukushima, K., Fujishima, M., Herr, W., Nishimoto, T., 1997. A single-point mutation in HCF causes temperature-sensitive cell-cycle arrest and disrupts VP16 function. *Genes Dev.* 11, 726–737.
- Hadjantonakis, A.K., Cox, L.L., Tam, P.P., Nagy, A., 2001. An X-linked GFP transgene reveals unexpected paternal X-chromosome activity in trophoblastic giant cells of the mouse placenta. *Genesis* 29, 133–140.
- Hadjantonakis, A.K., Gertsenstein, M., Ikawa, M., Okabe, M., Nagy, A., 1998. Non-invasive sexing of preimplantation stage mammalian embryos. *Nat. Genet.* 19, 220–222.
- Hayashi, S., Lewis, P., Pevny, L., McMahon, A.P., 2002. Efficient gene modulation in mouse epiblast using a Sox2Cre transgenic mouse strain. *Mech. Dev.* 119 (Suppl. 1), S97–S101.
- Hayashi, S., Tenzen, T., McMahon, A.P., 2003. Maternal inheritance of Cre activity in a Sox2Cre deleter strain. *Genesis* 37, 51–53.
- Heard, E., Distech, C.M., 2006. Dosage compensation in mammals: fine-tuning the expression of the X chromosome. *Genes Dev.* 20, 1848–1867.
- Huang, L., Jolly, L.A., Willis-Owen, S., Gardner, A., Kumar, R., Douglas, E., Shoubridge, C., Wieczorek, D., Tzschach, A., Cohen, M., Hackett, A., Field, M., Froyen, G., Hu, H., Haas, S.A., Ropers, H.H., Kalscheuer, V.M., Corbett, M.A., Gecz, J., 2012. A noncoding, regulatory mutation implicates HCF1 in nonsyndromic intellectual disability. *Am. J. Hum. Genet.* 91, 694–702.
- Johnson, K.M., Mahajan, S.S., Wilson, A.C., 1999. Herpes simplex virus transactivator VP16 discriminates between HCF-1 and a novel family member, HCF-2. *J. Virol.* 73, 3930–3940.
- Joyner, A., Wall, N., 2008. Immunohistochemistry of whole-mount mouse embryos. *CSH Protoc.* 2008, pdb prot4820.
- Julien, E., Herr, W., 2003. Proteolytic processing is necessary to separate and ensure proper cell growth and cytokinesis functions of HCF-1. *EMBO J.* 22, 2360–2369.
- Kelman, Z., 1997. PCNA: structure, functions and interactions. *Oncogene* 14, 629–640.
- Kristie, T.M., 1997. The mouse homologue of the human transcription factor C1 (host cell factor). Conservation of forms and function. *J. Biol. Chem.* 272, 26749–26755.
- Kristie, T.M., Liang, Y., Vogel, J.L., 2010. Control of alpha-herpesvirus IE gene expression by HCF-1 coupled chromatin modification activities. *Biochim. Biophys. Acta* 1799, 257–265.
- Le, Y., Sauer, B., 2000. Conditional gene knockout using cre recombinase. *Methods Mol. Biol.* 136, 477–485.
- Longo, L., Vanegas, O.C., Patel, M., Rosti, V., Li, H., Waka, J., Merghoub, T., Pandolfi, P., Notaro, R., Manova, K., Luzzatto, L., 2002. Maternally transmitted severe glucose 6-phosphate dehydrogenase deficiency is an embryonic lethal. *EMBO J.* 21, 4229–4239.
- Mak, W., Nesterova, T.B., de Napoles, M., Appanah, R., Yamanaka, S., Otte, A.P., Brockdorff, N., 2004. Reactivation of the paternal X chromosome in early mouse embryos. *Science* 303, 666–669.
- Martinez Arias, A., Nichols, J., Schroter, C., 2013. A molecular basis for developmental plasticity in early mammalian embryos. *Development* 140, 3499–3510.
- McBurney, M.W., Staines, W.A., Boekelheide, K., Parry, D., Jardine, K., Pickavance, L., 1994. Murine PGK-1 promoter drives widespread but not uniform expression in

- transgenic mice. *Dev. Dyn.* 200, 278–293.
- McMahon, A., Fosten, M., Monk, M., 1983. X-chromosome inactivation mosaicism in the three germ layers and the germ line of the mouse embryo. *J. Embryol. Exp. Morphol.* 74, 207–220.
- Michalopoulos, G.K., DeFrances, M.C., 1997. Liver regeneration. *Science* 276, 60–66.
- Michaud, J., Praz, V., James Faresse, N., Jnbaptiste, C.K., Tyagi, S., Schutz, F., Herr, W., 2013. HCF1 is a common component of active human CpG-island promoters and coincides with ZNF143, THAP11, YY1, and GABP transcription factor occupancy. *Genome Res.* 23, 907–916.
- Mitchell, C., Willenbring, H., 2008. A reproducible and well-tolerated method for 2/3 partial hepatectomy in mice. *Nat. Protoc.* 3, 1167–1170.
- O'Donnell, N., Zachara, N.E., Hart, G.W., Marth, J.D., 2004. Ogt-dependent X-chromosome-linked protein glycosylation is a requisite modification in somatic cell function and embryo viability. *Mol. Cell. Biol.* 24, 1680–1690.
- Park, J., Lammers, F., Herr, W., Song, J.J., 2012. HCF-1 self-association via an interdigitated Fn3 structure facilitates transcriptional regulatory complex formation. *Proc. Natl. Acad. Sci. USA* 109, 17430–17435.
- Power, M.A., Tam, P.P., 1993. Onset of gastrulation, morphogenesis and somitogenesis in mouse embryos displaying compensatory growth. *Anat. Embryol.* 187, 493–504.
- Prigent, C., Dimitrov, S., 2003. Phosphorylation of serine 10 in histone H3, what for? *J. Cell Sci.* 116, 3677–3685.
- Rands, G.F., 1986. Size regulation in the mouse embryo. II. The development of half embryos. *J. Embryol. Exp. Morphol.* 98, 209–217.
- Rastan, S., 1982. Timing of X-chromosome inactivation in postimplantation mouse embryos. *J. Embryol. Exp. Morphol.* 71, 11–24.
- Reilly, P.T., Herr, W., 2002. Spontaneous reversion of tsBN67 cell proliferation and cytokinesis defects in the absence of HCF-1 function. *Exp. Cell Res.* 277, 119–130.
- Reilly, P.T., Wysocka, J., Herr, W., 2002. Inactivation of the retinoblastoma protein family can bypass the HCF-1 defect in tsBN67 cell proliferation and cytokinesis. *Mol. Cell. Biol.* 22, 6767–6778.
- Scholzen, T., Gerdes, J., 2000. The Ki-67 protein: from the known and the unknown. *J. Cell. Physiol.* 182, 311–322.
- Schuler, M., Dierich, A., Chambon, P., Metzger, D., 2004. Efficient temporally controlled targeted somatic mutagenesis in hepatocytes of the mouse. *Genesis* 39, 167–172.
- Snow, M.H., Tam, P.P., 1979. Is compensatory growth a complicating factor in mouse teratology? *Nature* 279, 555–557.
- Steele-Perkins, G., Plachez, C., Butz, K.G., Yang, G., Bachurski, C.J., Kinsman, S.L., Litwack, E.D., Richards, L.J., Gronostajski, R.M., 2005. The transcription factor gene *Nfib* is essential for both lung maturation and brain development. *Mol. Cell. Biol.* 25, 685–698.
- Sulston, J.E., Schierenberg, E., White, J.G., Thomson, J.N., 1983. The embryonic cell lineage of the nematode *Caenorhabditis elegans*. *Dev. Biol.* 100, 64–119.
- Tam, P.P., 1988. Postimplantation development of mitomycin C-treated mouse blastocysts. *Teratology* 37, 205–212.
- Taub, R., 2004. Liver regeneration: from myth to mechanism. *Nat. Rev. Mol. Cell Biol.* 5, 836–847.
- Truett, G.E., Heeger, P., Mynatt, R.L., Truett, A.A., Walker, J.A., Warman, M.L., 2000. Preparation of PCR-quality mouse genomic DNA with hot sodium hydroxide and tris (HotSHOT). *BioTechniques* 29 (52), 54.
- Vincent, S.D., Robertson, E.J., 2003. Highly efficient transgene-independent recombination directed by a maternally derived SOX2CRE transgene. *Genesis* 37, 54–56.
- Wilson, A.C., Freiman, R.N., Goto, H., Nishimoto, T., Herr, W., 1997. VP16 targets an amino-terminal domain of HCF involved in cell cycle progression. *Mol. Cell. Biol.* 17, 6139–6146.
- Wilson, A.C., LaMarco, K., Peterson, M.G., Herr, W., 1993. The VP16 accessory protein HCF is a family of polypeptides processed from a large precursor protein. *Cell* 74, 115–125.
- Wilson, A.C., Parrish, J.E., Massa, H.F., Nelson, D.L., Trask, B.J., Herr, W., 1995. The gene encoding the VP16-accessory protein HCF (HCF1) resides in human Xq28 and is highly expressed in fetal tissues and the adult kidney. *Genomics* 25, 462–468.
- Wysocka, J., Reilly, P.T., Herr, W., 2001. Loss of HCF-1-chromatin association precedes temperature-induced growth arrest of tsBN67 cells. *Mol. Cell. Biol.* 21, 3820–3829.
- Zargar, Z., Tyagi, S., 2012. Role of host cell factor-1 in cell cycle regulation. *Transcription* 3, 187–192.